

TR(BR)-3/1999-2000

## APPLICATION OF SCS-CN BASED RUNOFF MODEL



**NATIONAL INSTITUTE OF HYDROLOGY  
JAL VIGYAN BHAWAN  
ROORKEE - 247 667 (INDIA)**

## PREFACE

The process of storm runoff generation being too complex has been of concern to hydrologists, engineers, researchers, and planners since long. Methods ranging from the simple empirical fits to the time and space distributed models are available in literature. In practice, the linear unit hydrograph concept and its variations along with a mechanism for accounting for infiltration losses are generally used for runoff computation. The Soil Conservation Curve Number (SCS-CN) method developed in 1956 is widely used, for it accounts for major runoff producing physical characteristics of watersheds in terms of soil, land use, hydrologic condition, and antecedent moisture condition.

In this report, a time distributed SCS-CN based runoff method is developed and applied to several rainfall-runoff events of two watersheds. Methodology is described in steps for ease in hand computation and the application is described using examples, for practising/field engineers.

The report entitled 'Application of SCS-CN based runoff model' has been prepared by Dr. Surendra Kumar Mishra, Scientist E and Divisional Head, Flood Studies Division, National Institute of Hydrology Roorkee. I hope the contents of the report will be useful not only to academicians, research scholars but also to field and practising engineers.

  
DR. S.M. SETH  
DIRECTOR

## **CONTENTS**

<b>Preface</b>	
<b>List of Figures</b>	<b>(i)</b>
<b>List of Tables</b>	<b>(ii)</b>
<b>Abstract</b>	<b>(iii)</b>
<b>INTRODUCTION</b>	<b>1</b>
<b>SCS-CN METHOD</b>	<b>3</b>
<b>DERIVATION OF SCS-CN BASED RUNOFF METHOD</b>	<b>7</b>
<b>STUDY WATERSHEDS</b>	<b>11</b>
<b>APPLICATION</b>	<b>16</b>
<b>CONCLUSION</b>	<b>52</b>
<b>REFERENCES</b>	<b>53</b>

### LIST OF FIGURES

Fig. No.	Title	Page No.
1	Index map of Jhandoo Nala watershed	12
2	Map of 3F sub-zone watershed of Lower Godavary	14
3	Flow chart of the model	16
4	Rainfall-runoff simulation of event 1 of Himalayan Jhandoo Nala watershed	20
5	Rainfall-runoff simulation of event 2 of Himalayan Jhandoo Nala watershed	21
6	Rainfall-runoff simulation of event 3 of Himalayan Jhandoo Nala watershed	22
7	Rainfall-runoff simulation of event 4 of Himalayan Jhandoo Nala watershed	23
8	Rainfall-runoff simulation of event 5 of Himalayan Jhandoo Nala watershed	24
9	Rainfall-runoff simulation of event 6 of Himalayan Jhandoo Nala watershed	25
10	Rainfall-runoff simulation of event 7 of Himalayan Jhandoo Nala watershed	26
11	Rainfall-runoff simulation of event 8 of Himalayan Jhandoo Nala watershed	27
12	Rainfall-runoff simulation of event 9 of Himalayan Jhandoo Nala watershed	28
13	Rainfall-runoff simulation of event 10 of Himalayan Jhandoo Nala watershed	29
14	Rainfall-runoff simulation of event 11 of Himalayan Jhandoo Nala watershed	30
15	Rainfall-runoff simulation of event 12 of Himalayan Jhandoo Nala watershed	31
16	Rainfall-runoff simulation of event 13 of Himalayan Jhandoo Nala watershed	32
17	Rainfall-runoff simulation of event 14 of Himalayan Jhandoo Nala watershed	33
18	Rainfall-runoff simulation of event 15 of Himalayan Jhandoo Nala watershed	34
19	Rainfall-runoff simulation of event 16 of Himalayan Jhandoo Nala watershed	35
20	Rainfall-runoff simulation of event 17 of Himalayan Jhandoo Nala watershed	36
21	Rainfall-runoff simulation of event 1 of Godavary basin	37
22	Rainfall-runoff simulation of event 2 of Godavary basin	38
23	Rainfall-runoff simulation of event 3 of Godavary basin	39
24	Rainfall-runoff simulation of event 4 of Godavary basin	40
25	Rainfall-runoff simulation of event 5 of Godavary basin	41
26	Rainfall-runoff simulation of event 6 of Godavary basin	42
27	Rainfall-runoff simulation of event 7 of Godavary basin	43

### LIST OF TABLES

Table No.	Title	Page No.
1	Simulation of rainfall-runoff events of Jhandoo Nala watershed	18
2	Simulation of rainfall-runoff events of 3F sub-zone watershed of Godavary	19
3	Volumetric statistics of the rainfall-runoff events of Jhandoo Nala watershed	46
4	Volumetric statistics of the rainfall-runoff events of 3F sub-zone watershed of Godavary	47
5	An example application of the model for event 3 of Jhandoo Nala watershed	48
6	An example application of the model for event 1 of 3F sub-zone watershed of Godavary	49
7	Variation of curve number within an example event (Event 1 of Jhandoo Nala watershed)	51

## ABSTRACT

Modelling of rainfall generated runoff is of paramount importance in hydrological design of water resources structures. The Soil Conservation Service (1956, 1964, 1985) Curve Number (SCS-CN) method is most popularly used by scientists, engineers, practitioners, and academicians, for it is simple, stable, and takes into account most of the watershed's runoff producing characteristics: soil type, land use, hydrologic condition, and antecedent moisture condition. This event-based spatially and temporally lumped method has also been used in long term hydrologic simulation with varying degree of success. The present report develops a spatially lumped but temporally distributed SCS-CN based runoff model for simulating seventeen rainfall-runoff events of a mine-affected Himalayan Jhandoo Nala watershed (area=17.7 ha) and seven events of 3F sub-zone watershed (area = 823.62 sq. km) of Godavary. The application of the developed methodology has also been demonstrated with the help of two examples. Simulation results are discussed with the help of error criteria of standard error and coefficient of determination, for evaluating the model performance, and relative error is used for evaluating the model performance in simulating the volumes of the runoffs. It is found that peak discharges and time to peak discharges simulate reasonably well and mass is conserved satisfactorily.

## INTRODUCTION

Rainfall-runoff modelling is an important and integral part of the water resources planning and management. The long term hydrologic simulation is important for water availability studies (Ponce and Hawkins, 1996) whereas short term modelling for the estimation of flood peaks for designing flood protection and management works. Linear convolution techniques, for example unit hydrograph, coupled with a mechanism, such as  $\phi$ -index, for accounting infiltration losses are generally employed for rainfall-runoff simulation. However, the sophisticated and advanced distributed watershed models, for example, System Hydrologic European (SHE) model, utilise infiltration models along with others for computing the runoff. In this report, spatially lumped and temporally distributed event-based (or short-term) simulation is attempted using the Soil Conservation Service-Curve Number (SCS-CN) method (Soil Conservation Service, 1956, 1964, 1987).

The SCS-CN method is one of the most popular methods for computing the volume of surface runoff for a given rainfall event from small agricultural watersheds. The method has been the focus of much discussion in agricultural hydrologic literature. In a very recent article, Ponce and Hawkins (1996) critically examined this method; clarified its conceptual and empirical basis; delineated its capabilities, limitations, and uses; and identified areas of research in the SCS-CN methodology.

The origin of the SCS-CN method can be traced to the proposal of Sherman (1942, 1949) on plotting direct runoff versus storm rainfall, and the subsequent work of Mockus (1949) on estimation of surface runoff for ungauged watersheds using information on soil, land use, antecedent rainfall, storm duration, and average annual temperature. Andrews (1954) developed a graphical procedure for estimating runoff from rainfall for combinations of soil texture and type, amount of vegetative cover, and conservation practices, all combined in what is referred to as soil-cover complex or soil-vegetation-land use (SVL) complex (Miller and Cronshey, 1989). Thus, the empirical rainfall-runoff relation of Mockus (1949) and the SVL complex of Andrews (1954)

constituted the building blocks of the SCS-CN method described in the Soil Conservation Service National Engineering Handbook Section 4 (Soil Conservation Service, 1956, 1985). Rallison and Miller (1982) succinctly described the SCS-CN method as a graphical transformation and generalisation of the works of Andrews (1954) and Mockus (1949).

There is a considerable amount of literature published on the SCS-CN method and several recent articles review much of this literature. For example, Ponce and Hawkins (1996) provided a good overview. Steenhuis et al. (1995) showed that the SCS method was based on the principles used in partial area hydrology and could predict the contributing area (Hewlett and Hibbert, 1967; Dunne and Black, 1970). Hawkins(1993) discussed determination of curve numbers from empirical data. Svoboda (1991) used the curve number concept to calculate the soil-water content and subsequently the rainfall contribution to direct runoff and groundwater. Hjelmfelt (1991) provided a comprehensive discussion of the method, including the heritage of the method, determination of curve numbers from rainfall-runoff data, and interpretation of antecedent moisture conditions. Ritter and Gardner (1991) discussed application of the SCS-CN method to watersheds located on reclaimed surface coal mines in Central Pennsylvania. Mishra (2000) developed an SCS-CN based long-term hydrologic model and applied to the data of three Indian catchments.

The objective of this report is to review SCS-CN method, develop an SCS-CN based runoff model for computing direct runoff that is routed using the single linear reservoir technique, and apply the developed model to seventeen events of the Jhandoo Nala watershed of Himalaya and seven events of 3F sub-zone watershed of Godavary.



## SCS-CN METHOD

The SCS-CN method is based on the water balance equation and two fundamental hypotheses. The first hypothesis states that the ratio of the actual amount of surface runoff to the maximum potential runoff is equal to the ratio of the amount of actual infiltration to the amount of the potential maximum retention. The second hypothesis states that the amount of initial abstraction is some fraction of the potential maximum retention. Expressed mathematically, the water balance equation and the two hypotheses, respectively, are:

$$P = I_a + F + Q \quad (1)$$

$$\frac{Q}{P - I_a} = \frac{F}{S} \quad (2)$$

$$I_a = \lambda S \quad (3)$$

where  $P$ = total rainfall;  $I_a$ = initial abstraction;  $F$ = cumulative infiltration excluding  $I_a$ ;  $Q$ = direct runoff; and  $S$ = potential maximum retention. The current version of the SCS-CN method assumes  $\lambda$  equal to 0.2 in routine applications and Mishra and Singh [1999a,b], however, found it to vary in the range  $(0, \infty)$ . It is to note that  $P=0$  leads to a trivial solution of Eq. 2 for  $S$ , for  $I_a=Q=F=0$ . Combination of Eqs. 1 and 2 leads to

$$Q = \frac{(P - I_a)^2}{P - I_a + S} \quad (4)$$

which is valid for  $P \geq I_a$ ,  $Q=0$  otherwise. The relation between  $S$  and CN is expressed as

$$S = \frac{1000}{CN} - 10 \quad (5)$$

Coupling of Eq. 4 with Eq. 3 yields

$$\lambda^2 (S/P)^2 - [2\lambda + (1 - \lambda)C](S/P) + 1 - C = 0 \quad (6a)$$

which solves for  $S/P$  as

$$\frac{S}{P} = \frac{[2\lambda + C(1 - \lambda)] \pm \sqrt{C[C(1 - \lambda)^2 + 4\lambda]}}{2\lambda^2} \quad (6)$$

where  $C=Q/P$ . Since the term in the square root of numerator of Eq. 6 is always greater than or equal to zero and is always less than the first bracketed term in numerator,  $S/P$

will always be a non-negative quantity. For  $S/P=0$ ,  $4\lambda^2(1-C)=0$ , therefore, either  $\lambda=0$  or  $C=1$ . From Eq. 6a  $C=1$  and, therefore,  $\lambda=0$  is invalid. Thus, for  $S/P=0$  (or  $S=0$  if  $P$  is taken to be a finite quantity), only '-' sign, as normally used, is valid in place of  $\pm$  sign in the equation. Furthermore, for  $S=0$ ,  $C=1$  (or  $Q=P$ ), implying that  $F=I_a=0$  (Eq. 1) under the condition that  $\lambda \neq 0$ . Thus,  $I_a$  is directly governed by  $S$ , consistent with the description of McCuen (1982). Since  $S$  represents the potential maximum retention,  $I_a$  should be characterised as the potential amount of initial abstraction. Eq. 6a or Eq. 6b, however, does not describe the range of  $\lambda$  variation. These can be explained using  $I_a$  as a descriptor of  $S$  [McCuen, 1982], in what follows [Mishra and Singh, 1999b].

Multiplication of Eq. 6 by 1 yields

$$I_a^* = \frac{[2\lambda + C(1-\lambda)] - \sqrt{C[C(1-\lambda)^2 + 4\lambda]}}{2\lambda} \quad (7)$$

where  $I_a^* = I_a/P$ . Eq. 7 can be utilised for describing the functional behaviour of SCS-CN method in  $C-I_a^*-\lambda$  space, for the reason that the variation of  $I_a^*$  has a range of  $0 \leq I_a^* \leq 1$  and if  $I_a^* > 1$ ,  $C=0$ . For the condition  $0 \leq I_a^* \leq 1$ , Eq. 7 yields  $\lambda \geq 0$  and  $0 \leq C \leq 1$  and is valid for only '-' sign before the square root in the numerator of Eq. 7 instead of ' $\pm$ ' sign. The solution of Eq. 7 for  $\lambda$  yields

$$\lambda = \frac{C I_a^*}{(1 - I_a^*)(1 - I_a^* - C)} \quad (8)$$

and  $\lambda=0$ . Eq. 8 is also directly derivable from Eq. 4. In Eq. 8, if  $I_a^* \rightarrow 1$  or  $(I_a^* + C) \rightarrow 1$ ,  $\lambda \rightarrow \infty$ . Eq. 8 yields prohibitive negative value of  $\lambda$  [ $= -1/(1-I_a^*)$ ] for  $C$  approaching 1. Thus, for  $\lambda$  to be a non-negative value, the following should hold

$$I_a^* + C \leq 1 \quad (9a)$$

or, alternatively,

$$Q + I_a \leq P \quad (9b)$$

As  $(I_a^* + C) \rightarrow P$  or  $I_a^* \rightarrow (1-C)$  or  $(1-I_a^*) \rightarrow C$ ,  $I_a^*/\lambda$  or  $S/P \rightarrow 0$  (Eq. 8), implying  $S \rightarrow 0$  for  $P$  is a finite quantity, as above, and  $\lambda \rightarrow \infty$ . Coupling of Eq. 9b with Eq. 1 yields  $F \geq 0$  and combination of Eq. 3 with Eq. 9b leads to

$$S \leq \frac{P-Q}{\lambda} \quad (10)$$

implying that  $S \leq 5(P-Q)$  for  $\lambda=0.2$ . The definition of maximum difference of  $(P-Q)$  (Mockus, 1964) (also described later) is a special case of  $\lambda=0$  or  $I_a=0$ .

For an additional insight into the SCS-CN method, three specific cases are considered. First, for an immediate ponding upon rainfall, an extreme case,  $I_a=0$ . Therefore, Eq. 4 reduces to

$$Q = \frac{P^2}{P+S} = \frac{P}{1+(S/P)} \quad (11a)$$

or

$$Q/P = [1 + (S/P)]^{-1} \quad (11b)$$

If  $S$  and  $P$  are equal, then  $Q=0.5P$ , i.e., the volume of surface runoff is half of the rainfall amount. Second, if  $I_a=S$ , Eq. 4 reduces to

$$Q = \frac{(P-S)^2}{P} = P \left(1 - \frac{S}{P}\right)^2 \quad (12)$$

If  $S=P$ ,  $Q=0$ , i.e., the entire rainfall is absorbed by the soil and consequently no surface runoff volume is produced. Finally, if  $I_a=P$ , then  $Q=0$ .

## DERIVATION OF SCS-CN BASED RUNOFF METHOD

The SCS-CN method can be construed as an infiltration loss model [Ponce and Hawkins, 1996]. Further analysis is to show analytically that the SCS-CN method, in approximate form, is an infiltration loss model. To this end, the Mockus [1949] method from which the SCS-CN method has been generalised is analysed. It is expressed mathematically as

$$Q = P_e [1 - 10^{-bP_e}] \quad (13)$$

where  $P_e$  is the effective rainfall ( $=P-I_s$ ) and  $b$  is a parameter. The basic underlying concept of Eq. 13 [Mishra and Singh, 1999a] is given below:

$$\frac{dF}{dP_e} = -B F \quad (14)$$

where  $B=1/S = b \cdot \ln(10)$ . Assuming that  $P_e$  grows linearly with time  $t$  as below:

$$P_e = i_e t \quad (15)$$

where  $i_e$  is a proportionality constant. Eq. 15 also asserts the general notion that  $P_e$  grows unbounded [Ponce and Hawkins, 1996]. Using first order finite difference (Ponce, 1989), Eq. 14 can be re-written for a time interval  $\Delta t = t_{j+1} - t_j, j = 1, 2, 3 \dots$  as:

$$\frac{F_{t+1} - F_t}{F_t} = -B (P_{e,t+1} - P_{e,t}) \quad (16)$$

or, alternatively,

$$F_{t+1} = F_t (1 - B \Delta P_e) \quad (17)$$

The concept underlying the SCS-CN method (Eq. 14) is analogous to the one employed for deriving the popular Horton's infiltration loss equation:

$$f = f_0 e^{-kt} \quad (18)$$

for the final infiltration rate  $f_c=0$ . The basic concept underlying Eq. 18 is

$$\frac{df}{dt} = -k f \quad (19)$$

where  $f$  is the infiltration rate,  $f_0$  is the initial infiltration rate at time  $t=0$ ,  $k$  is the decay constant ( $T^{-1}$ ). Eq. 19 can also be recast in the following form:

$$f_{t+1} = f_t (1 - k\Delta t) \quad (20)$$

Given the time interval  $\Delta t$ , the summation of the left hand side and the right hand side terms over time  $(t+1)$  leads to

$$F_{t+1} = F_t(1 - k \Delta t) + f_1 \Delta t \quad (21)$$

where  $F_t$  is the cumulative infiltration at time  $t$ . Similarly,  $F_{t+1}$  can be defined. Neglecting the term  $f_1 \Delta t$  in Eq. 21 leads to

$$F_{t+1} = F_t(1 - k \Delta t) \quad (22)$$

Eq. 22 is comparable to Eq. 17 and the comparison leads to an important relation:

$$P_e = \frac{k}{B} t = kSt \quad (23)$$

which is the same equation as Eq. 15. This yields the proportionality constant

$$i_e = kS \quad (24)$$

This, of course, is based on the assumption that  $P_e$  grows linearly with time. The absence of a term in Eq. 17 analogous to  $f_1 \Delta t$  in Eq. 21 limits the applicability of Eq. 14 and, in turn, the Mockus method (Eq. 13) to the time domain  $(t > 0)$ . Eq. 24 describes relationship among the three proportionality constants and defines Horton parameter  $k$  to be equal to the ratio of the effective rainfall intensity,  $i_e$ , to the potential maximum retention,  $S$ , implying that  $k$  increases as  $i_e$  increases and decreases as  $S$  increases or CN decreases, and vice versa also holds. Thus,  $k$  depends on the magnitude of effective rainfall intensity and soil type, land use, hydrologic condition, antecedent moisture that affect  $S$  and it is consistent, in general, with the description of Mein and Larson [1971]. Eq. 24 also permits derivation of the time distribution of infiltration rate and the time distribution of runoff from SCS-CN method. To this end, combining Eqs. 1 and 2, the SCS-CN equation is re-written for  $F$  as below:

$$F = \frac{P_e S}{P_e + S} \quad (25)$$

Coupling of Eq. 23 with Eq. 25 lead to

$$F = \frac{S k t}{(1 + kt)} \quad (26)$$

Differentiating Eq. 26 with respect to  $t$  and considering  $F$  to include  $f_c$  for generalisation gives

$$f = f_c + \frac{Sk}{(1+kt)^2} \quad (27)$$

Since the quantity (Sk) is constant, which is also equal to  $i_e$ , the effective rainfall intensity (Eq. 24),  $f$  decays with time. Analogous to the Horton equation Eq. 27 is also valid for  $i_e \geq f_c$ . Eq. 27 is the infiltration loss equation that is based on the SCS-CN method.

Similarly, the time distribution of the runoff hydrograph can be obtained as follows. Eq. 4 is recast as

$$Q = \frac{P_e^2}{S + P_e} \quad (28)$$

Replacing  $P_e$  by  $(kSt)$  in Eq. 28 gives

$$Q = \frac{S(k t)^2}{(1 + k t)} \quad (29)$$

For deriving incremental runoff, Eq. 29 can be differentiated as:

$$q = \frac{S k^2 t (2 + kt)}{(1 + kt)^2} \quad (30)$$

Multiplying Eq. 30 by the catchment area,  $A$ , gives the discharge  $q$  in the units,  $L^3T^{-1}$ , as:

$$q = \frac{A S k^2 t (2 + kt)}{(1 + kt)^2} \quad (31)$$

Replacing  $kS$  by  $i_e$  (Eq. 24) gives a more useful form of Eq. 31 as:

$$q = i_e A \left(1 - \frac{1}{(1 + k t)^2}\right) \quad (32)$$

which is a form of the continuity equation:

$$q = i_e A - f A \quad (33)$$

for  $f_c=0$ . In other words, the runoff rate is equal to the effective rainfall rate minus the rate of infiltration in volumetric units. Interpreted in hydrologic systems framework [Singh, 1988], Eq. 32 represents the response of two elements arranged in parallel. One of the elements is analogous to the reservoir (or storage element) underlying the rational method and the other element is an absorber representing infiltration.

Eq. 32 can also be written in dimensionless form

$$q^* = 1 - \frac{1}{(1 + k t)^2} \quad (34)$$

where  $q^* = q/(i_e A)$  = non-dimensional runoff rate at time  $t$  and  $i_e A$  = potential runoff.

For  $f_c$  greater than zero,  $q$  and  $q^*$  can be derived substituting Eq. 27 into Eq. 33, respectively, as

$$q = i_e A \left( 1 - \lambda_1 - \frac{1}{(1 + k t)^2} \right) \quad (35)$$

and

$$q^* = 1 - \lambda_1 - \frac{1}{(1 + k t)^2} \quad (36)$$

where  $\lambda_1 = f_c/i_e$  = the ratio of final infiltration rate to the effective rainfall intensity.

### Coupling of a Routing Mechanism with the Runoff Model

The runoff model (Eq. 35) is re-written for convenience below:

$$q = i_e A \left( 1 - \lambda_1 - \frac{1}{(1 + k t)^2} \right) \quad (35)$$

where  $i_e$  is the effective rainfall intensity and  $q$  is the rainfall excess at time  $t$ , which is routed to the outlet of the watershed using single linear reservoir, as follows:

Continuity equation:

$$\text{Inflow} - \text{Outflow} = \text{Rate of change in storage} \quad (37a)$$

$$q - Q = \Delta V / \Delta t \quad (37b)$$

Storage equation:

$$V = K Q \quad (38)$$

where  $V$  is the reservoir storage,  $K$  is the storage coefficient,  $\Delta t$  is the time interval, and  $Q$  is the outflow or runoff at the outlet or the routed flow. Using finite difference scheme,  $Q$  at different time steps can be computed as follows:

$$Q_{j+1} = d_1 q_j + d_2 Q_j \quad (39)$$

where  $Q$  is the routed runoff,  $q$  is the rainfall excess,  $J$  and  $J+1$  are the time steps, and

$$d_1 = \frac{1}{K/\Delta t + 0.5} \quad (40)$$

$$d_2 = \frac{K/\Delta t - 0.5}{K/\Delta t + 0.5} \quad (41)$$



## **STUDY WATERSHEDS**

The developed model has been applied to the data of two watersheds: Jhandoo Nala watershed and Godavary watershed, described below.

### **1. Jhandoo Nala Watershed**

#### **(i) Location**

The Jhandoo Nala watershed is located in Dehradun district near Sahastradhara in the Province of Uttar Pradesh (India) (Fig. 1). It is a sub-watershed of Kharawan-Dhandaula mined watershed located near Sastradhara. The Kharawan-Dhandaula watershed is 46 ha in area and has four sub-watersheds. This watershed is located between 32°23' and 32°23½' N latitude and between 78°7½' and 78°8' E longitude, at a distance of 14 km from Dehradun on Dehradun-Sahastradhara metalled road. This watershed is surrounded by lime stone mines in the north, Baldi river in the south, Sulphur spring in the east, and U.P. Forest Department Outpost in the west. The rainfall data were collected using a standard raingauge and a siphon type recording raingauge installed near the outlet of the watershed and the runoff data were collected from measurements on flume constructed at the outlet of the watershed. These data were used by Katiyar (1997) in his Ph.D. dissertation and are used in this study.

This watershed has been disturbed by lime-stone quarrying for about 30 years. The lime stone quarries at Mussoorie hills are located on very steep terrain. These mined areas are producing huge amount of debris including big sized boulders, chemical effluents and flash flows during monsoon season. This watershed used to produce sediment at the rate of 550 tonnes per hectare per year before treatment activities were taken up (Katiyar et al., 1987).

#### **(ii) Physiography**

The Jhandoo Nala watershed has an area of 17.7 hectares and ranges in elevation from 870 m to 1310 m with a relief of 440 m. Jhandoo Nala runs from north to south in

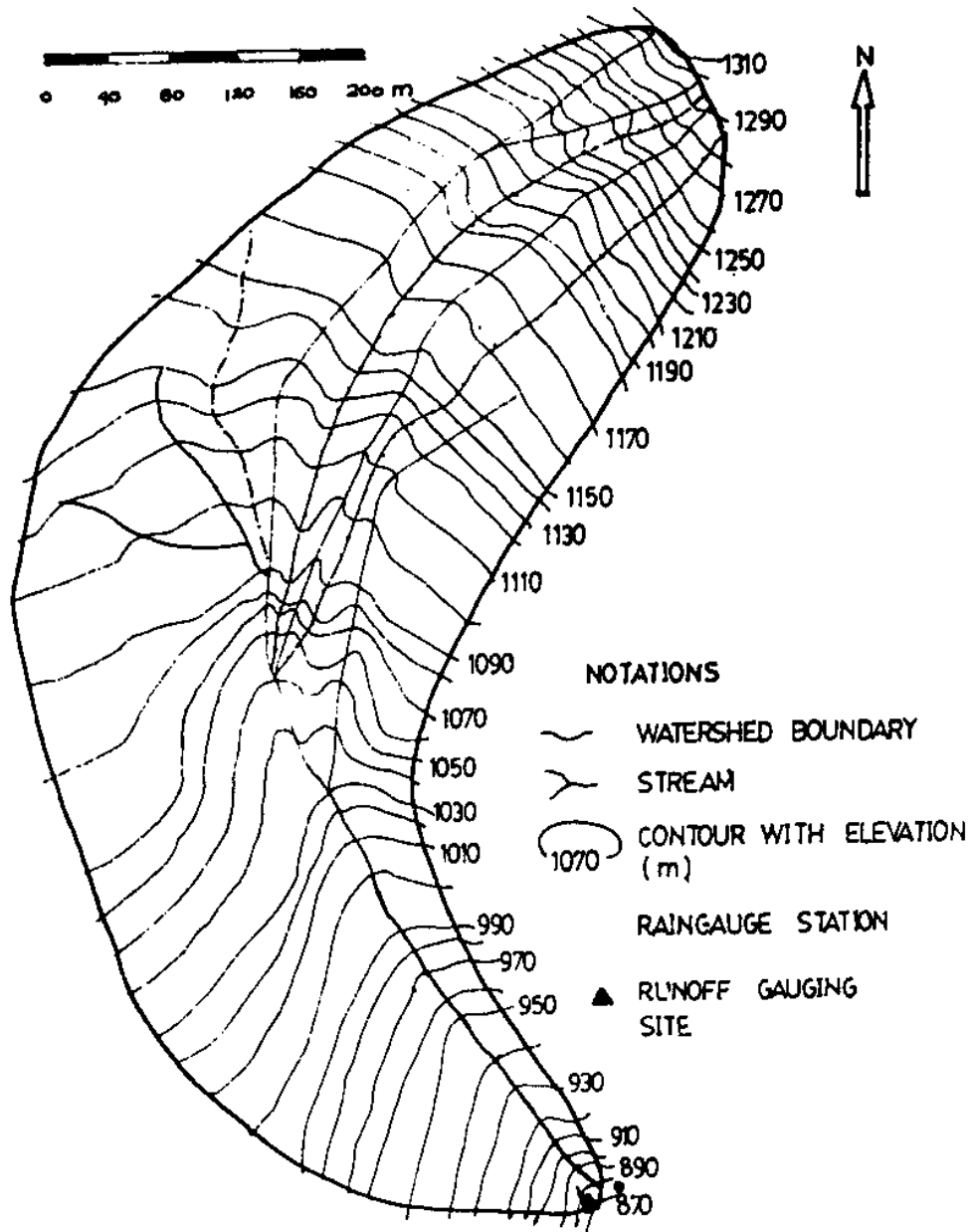


FIG.1. THE INDEX MAP OF JHANDOO NALA WATERSHED

the oblong shape. The average slope of the watershed is 60% for east aspect and 45% for west aspect, with an overall average of 50%. The area comprises of exposed cut rock surfaces, mine spoil/debris flows directly to Baldi river, a tributary of Ganges.

**(iii) Climate**

The watershed lies in sub-tropical zone. The average rainfall of the watershed is 2624 mm computed from the observed data from 1984-85 to 1993-94. The 88% of the annual rainfall is recorded in monsoon period. May is the hottest month with average maximum temperature of 38.2 °C and the average monthly minimum temperature, based on December and January, of 3.6 °C. The wind velocity varies from 1.1. to 3.4 km per hour.

**(iv) Soils**

Soils of the watershed vary from sandy loam to silty clay loam. The gravel percentage of these soils vary from 30 to 80%. Soils are very loose (porous) due to the use of dynamic explosions for mining of lime stone.

**(v) Land use**

The watershed was dominated by forest before mining works started, converting the major portion the watershed to a wasteland. About 0.76 ha land is now under cultivation (rainfed), 8.35 ha is wasteland, and 8.60 ha is scrub of medium canopy.

**2. 3F Sub-Zone Watershed of Godavary**

The 3F sub-zone watershed of lower Godavary river extends up to Bridge No. 807/1, as shown in Fig. 2. Sub-sone 3F of Godavary and its tributaries cover about 56% of the total catchment area (=823.62 sq. km) of the main Godavary river. This sub-zone covers the States of Maharashtra, Andhra Pradesh, and Orissa. It is spread between 17° and 23° N latitudes and between 76° and 83° E longitudes in L-shape.



FIG. 2. LOWER GODAVARI SUB ZONE 3(f)

The 3F sub-zone of lower Godavari falls mainly in humid region of India. Its average rainfall is of the order of 1300 mm. The main soil types of the watershed are red loamy sand and black soil; 50% of the area of the watershed is covered by forest, 25% by cultivated land, and the remaining 25% by barren land. The hourly rainfall and runoff data available with the Central Water Commission, New Delhi, were compiled by Tyagi et al. (1995) and these data are used in this study.

## APPLICATION

### a) Steps for Model Application

The methodology developed in the previous chapter is applied in the following steps (illustrated in Fig. 3):

1. Neglecting the initial abstraction, compute uniform rainfall intensity for the time duration taken from zero. For example, if  $i_1, i_2, i_3, \dots, i_n$  are the rainfall intensities in mm/hr, where 1, 2, 3 ...n. represent time steps at  $\Delta t$  time interval (hr). The uniform rainfall intensity ( $i_o$ ) at the  $n^{\text{th}}$  time step will be

$$i_o = (i_1 + i_2 + i_3 + \dots + i_n)/n \quad (42)$$

2. Taking  $S_k = i_o$ , compute infiltration rate  $f$  from Eq. 27 as follows:

$$f = f_c + \frac{i_o}{(1 + k.n\Delta t)^2} \quad (43)$$

where  $f$  and  $f_c$  are in mm/hr, and  $k$  is in  $\text{hr}^{-1}$ . If  $f > i_n$ , then  $f = i_n$ .

3. Compute rainfall excess  $q$  from continuity equation 33 as

$$q = (i_o - f) A/3.6 \quad (44)$$

where  $A$  is the catchment area in sq. km and  $q$  in cumec. If  $q < 0$ , then  $Q = 0$ .

4. Assuming  $Q_0 = 0$ ,  $Q_n$  can be computed from Eq. 39 as

$$Q_n = d_1 q_{n-1} + d_2 Q_{n-1} \quad (45)$$

where  $Q$ 's are in cumec.

5. Add baseflow, if any, to  $Q_n$  for computing total outflow (cumec).

6. Repeat steps 1 through 5 for computing the total runoff.

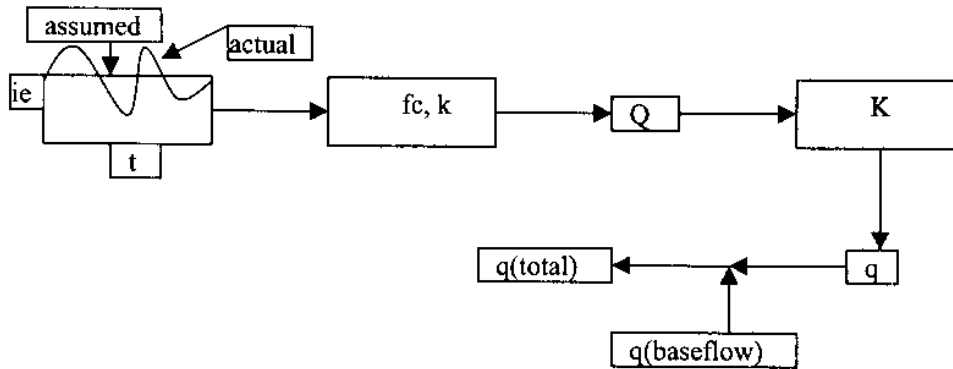


Fig. 3. Flow chart of the model.

In Fig. 3, the actual rainfall is averaged for each time step for the reason of uniform storm rainfall intensity ( $i_c$ ) used in the SCS-CN-based infiltration model (parameters:  $f_c$ ,  $k$ ). The computed rainfall excess ( $Q$ ) is routed through a single reservoir of  $K$  storage coefficient to obtain  $q$ , which when added to baseflow ( $q_{\text{baseflow}}$ ) leads to total flow ( $q_{\text{total}}$ ) at the outlet of the basin.

#### b) Details of Storm Events

The above model is applied to seventeen rainfall-runoff events of Jhandoo Nala watershed and seven events of 3F Sub-zone watershed of Godavary river. The details of the events along with the simulated results are given in Tables 1 and 2 for Jhandoo Nala and 3F sub-zone watersheds, respectively, and the simulated results are depicted graphically in Figs. 4 through 27. It is apparent from Table 1 and the corresponding Figs. 4 through 20 that the peak discharges of the events vary from 0.0455 to 0.4567 cumecs, time to peak from 20 to 230 min, baseflow from 0.0013 to 0.1383 cumecs, and the time base ranges between 180 and 360 min.

#### c) Error Criterion

The model parameters were computed using Marquardt algorithm of least squares using the criteria of standard error (SE) and coefficient of determination ( $r^2$ ), as given below:

$$SE = \sqrt{\sum_{i=1}^N (Q_o - Q_c)_i^2 / (N - m + 1)} \quad (46)$$

and

$$r^2 = 1 - \frac{\sum_{i=1}^N (Q_o - Q_c)_i^2}{\sum_{i=1}^N (Q_o - Q_m)_i^2} \quad (47)$$

TABLE 1. SIMULATION OF RAINFALL-RUNOFF EVENTS OF JHANDOO NALA WATERSHED

Event No.	Date	Runoff Characteristics			Optimized Parameters				Computed Runoff		Standard Error (cumec)	Coeff. of Determination ( $r^2$ )
		Peak discharge (cumec)	Time to peak discharge (min)	Baseflow (cumec)	Time base (min)	k ( $\text{min}^{-1}$ )	K (min)	$f_c$ (cumec)	Peak discharge (cumec)	Time to peak discharge (min)		
1	04.07.1990	0.1500	30	0.0255	270	$7.57 \times 10^{-4}$	3.95	0.0185	0.1609	40	0.0140	0.8341
2	16.08.1990	0.1760	50	0.0272	180	$4.87 \times 10^{-4}$	2.26	0.0141	0.1668	50	0.0234	0.7015
3	16.08.1990	0.0455	100	0.0272	300	$3.58 \times 10^{-4}$	22.40	0.0190	0.1523	150	0.0133	0.8668
4	25.08.1990	0.0827	80	0.0094	180	$2.94 \times 10^{-4}$	20.70	0.0005	0.0863	80	0.0097	0.8735
5	05.07.1991	0.0907	230	0.0013	360	$1.00 \times 10^{-4}$	26.80	0.0069	0.0821	240	0.0057	0.9252
6	07.08.1991	0.2933	110	0.0127	300	$2.84 \times 10^{-4}$	5.92	0.0000	0.2681	110	0.0472	0.5672
7	08.08.1991	0.4127	20	0.0647	240	$4.34 \times 10^{-3}$	2.43	0.0777	0.1612	70	0.0391	0.7901
8	09.08.1991	0.3777	40	0.0647	180	$9.98 \times 10^{-4}$	4.80	0.0000	0.2450	40	0.0497	0.6138
9	15.08.1991	0.2480	150	0.0073	240	$2.63 \times 10^{-4}$	25.60	0.0006	0.1952	150	0.0227	0.9001
10	16.08.1991	0.3313	40	0.0647	300	$7.80 \times 10^{-4}$	4.90	0.0000	0.3008	90	0.0503	0.5393
11	22.07.1992	0.4567	100	0.0272	360	$1.02 \times 10^{-2}$	19.80	1.4500	0.4551	100	0.0136	0.9782
12	17.07.1993	0.1656	70	0.0052	210	$4.36 \times 10^{-4}$	8.52	0.0000	0.1476	70	0.0201	0.8083
13	22.07.1993	0.1035	220	0.0367	300	$1.31 \times 10^{-4}$	27.00	0.0035	0.1099	220	0.0056	0.9148
14	02.08.1993	0.0528	50	0.0075	180	$2.27 \times 10^{-4}$	20.00	0.0073	0.0471	50	0.0031	0.9405
15	25.08.1993	0.2120	160	0.0477	300	$7.83 \times 10^{-3}$	0.18	0.0000	0.1524	160	0.0375	0.3975
16	29.08.1993	0.7878	50	0.1383	270	$1.19 \times 10^{-3}$	0.13	0.0000	0.1509	110	0.0681	0.7730
17	02.09.1993	0.3667	190	0.0127	330	$4.02 \times 10^{-3}$	99.40	0.3680	0.2858	190	0.0316	0.9187



**TABLE 2. SIMULATION OF RAINFALL-RUNOFF EVENTS OF 3F SUB-ZONE WATERSHED OF GODAVARY**

Event No.	Runoff Characteristics			Optimized Parameters			Computed Runoff		Standard Error (cumec)	Coeff. of Determination ( $r^2$ )	
	Peak discharge (cumec)	Time to peak discharge (hr)	Baseflow (cumec)	Time base (hr)	k ( $hr^{-1}$ )	K (hr)	$f_c$ (cumec)	Peak discharge (cumec)			Time to peak discharge (hr)
1	600	9	6.64	25	0.1710	3.89	108	385.37	8	75.68	0.8159
2	440	10	15.60	20	0.0717	8.82	0	322.20	8	69.63	0.7457
3	255	11	0.00	26	0.1090	6.22	252	150.38	9	44.53	0.6474
4	370	8	47.30	21	0.1530	5.17	0	193.36	5	86.23	0.4394
5	455	8	0.00	24	0.0573	7.38	0	253.75	6	76.84	0.6656
6	315	10	99.40	24	0.1140	6.85	294	175.12	9	81.75	0.2976
7	1432	7	0.00	23	0.2920	6.11	1080	966.35	8	194.72	0.7888

Source: Tyagi et al. (1995)

Fig. 4 Rainfall-runoff simulation of event 1 of Himalayan Jhandoo Nala watershed.

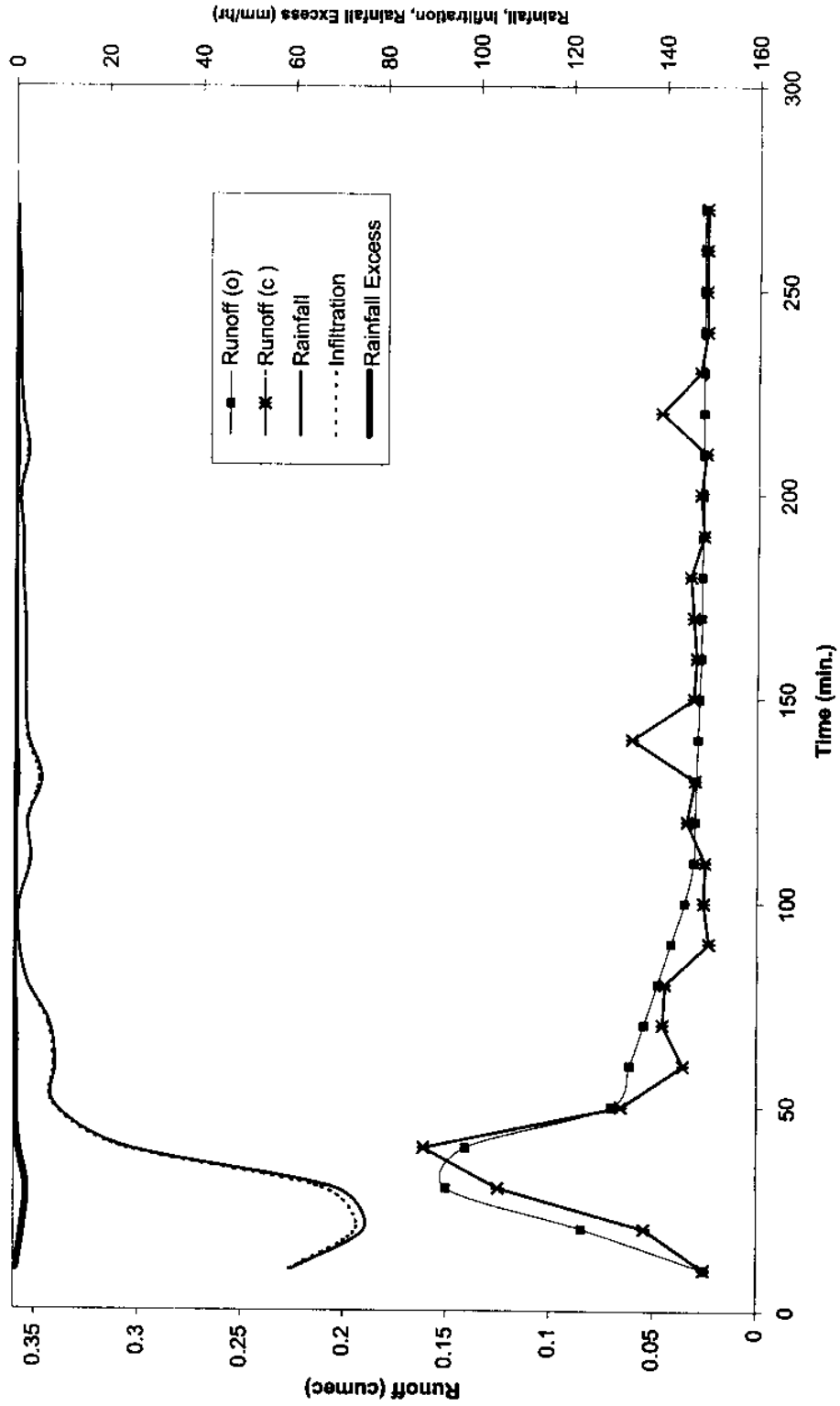


Fig. 5. Rainfall-runoff simulation of event 2 of Himalayan Jhandoo Nala watershed.

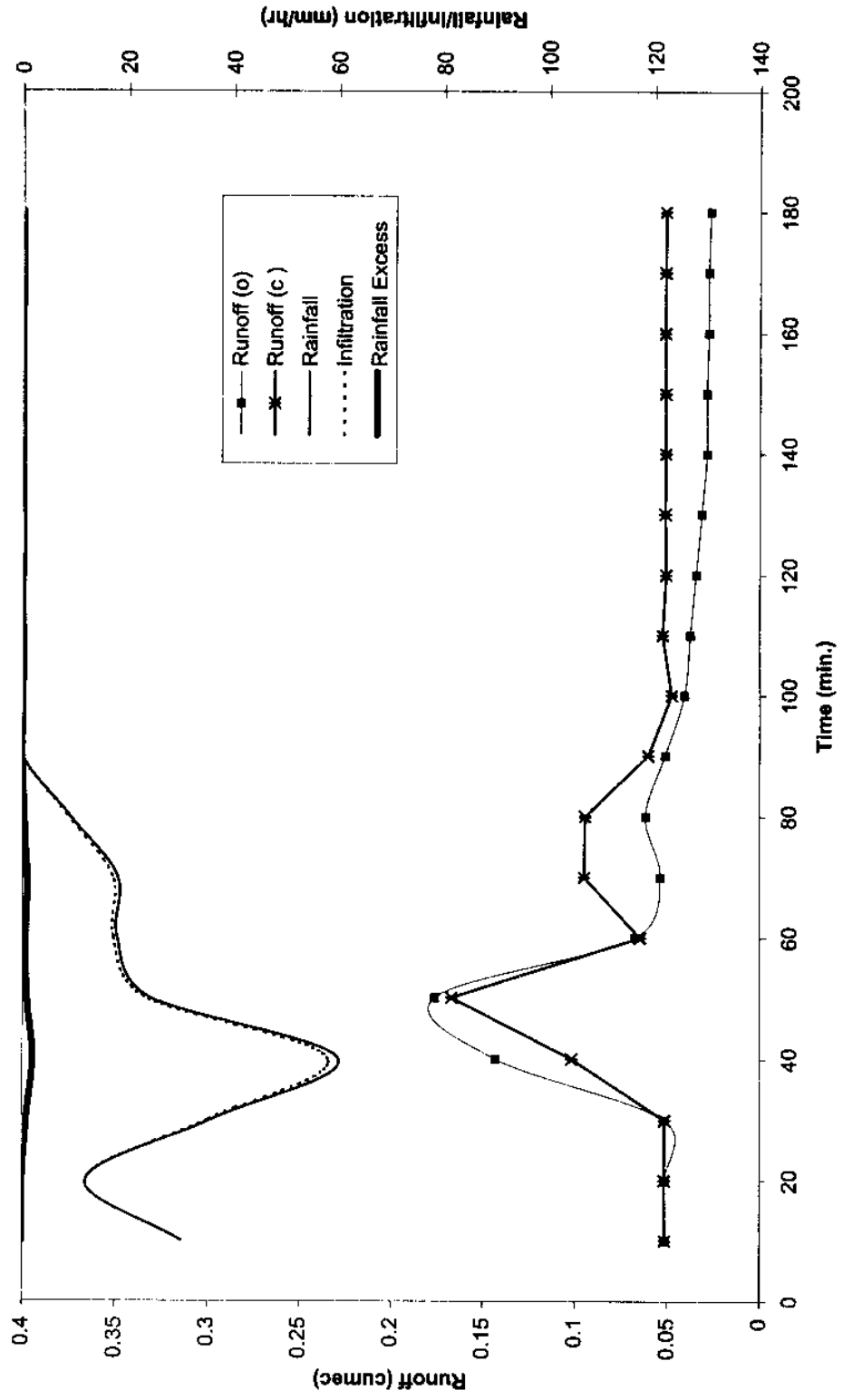


Fig. 6. Rainfall-runoff simulation of event 3 of Himalayan Jhandoo Nala watershed.

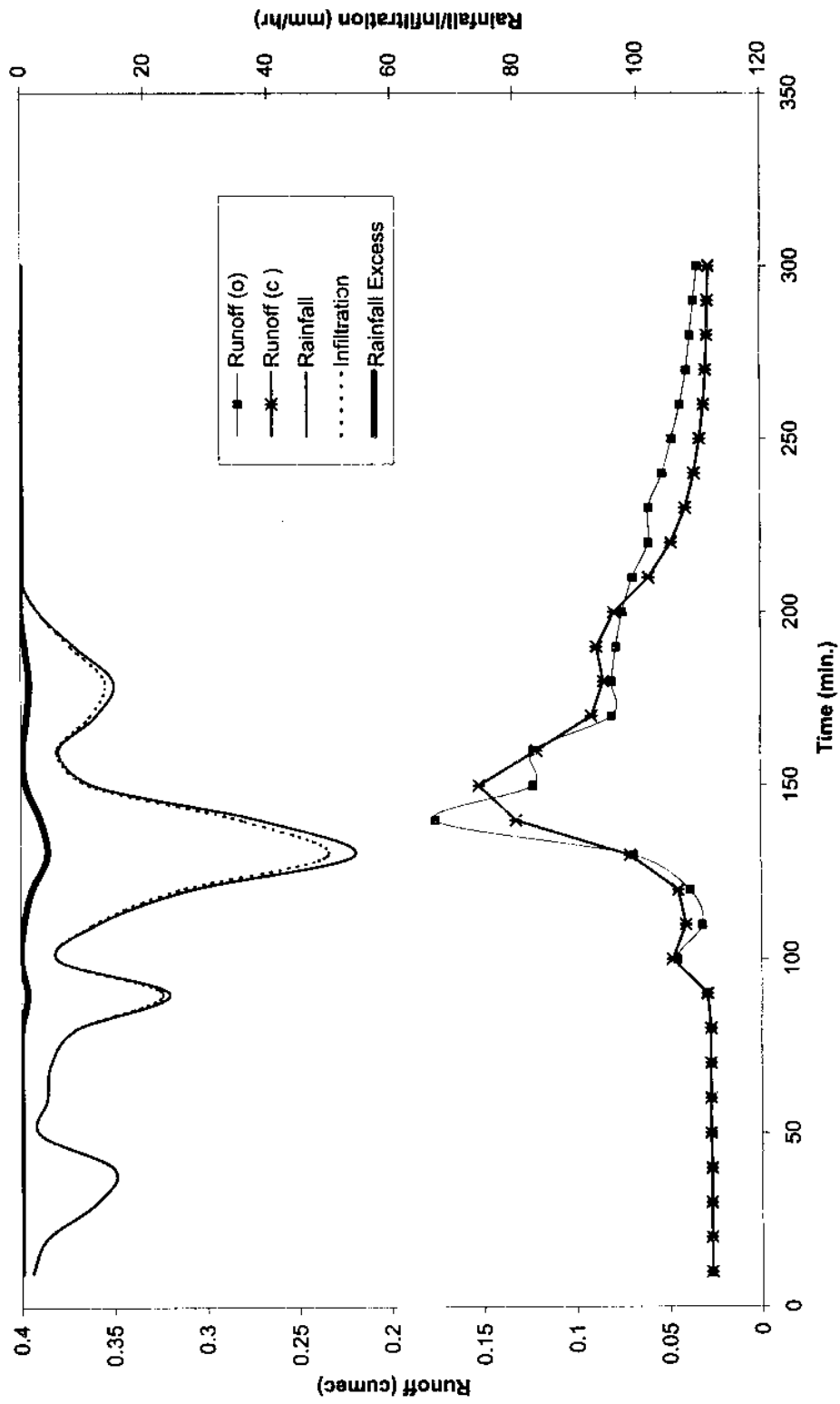


Fig. 7. Rainfall-runoff simulation of event 4 of Himalayan Jhandoo Nala watershed.

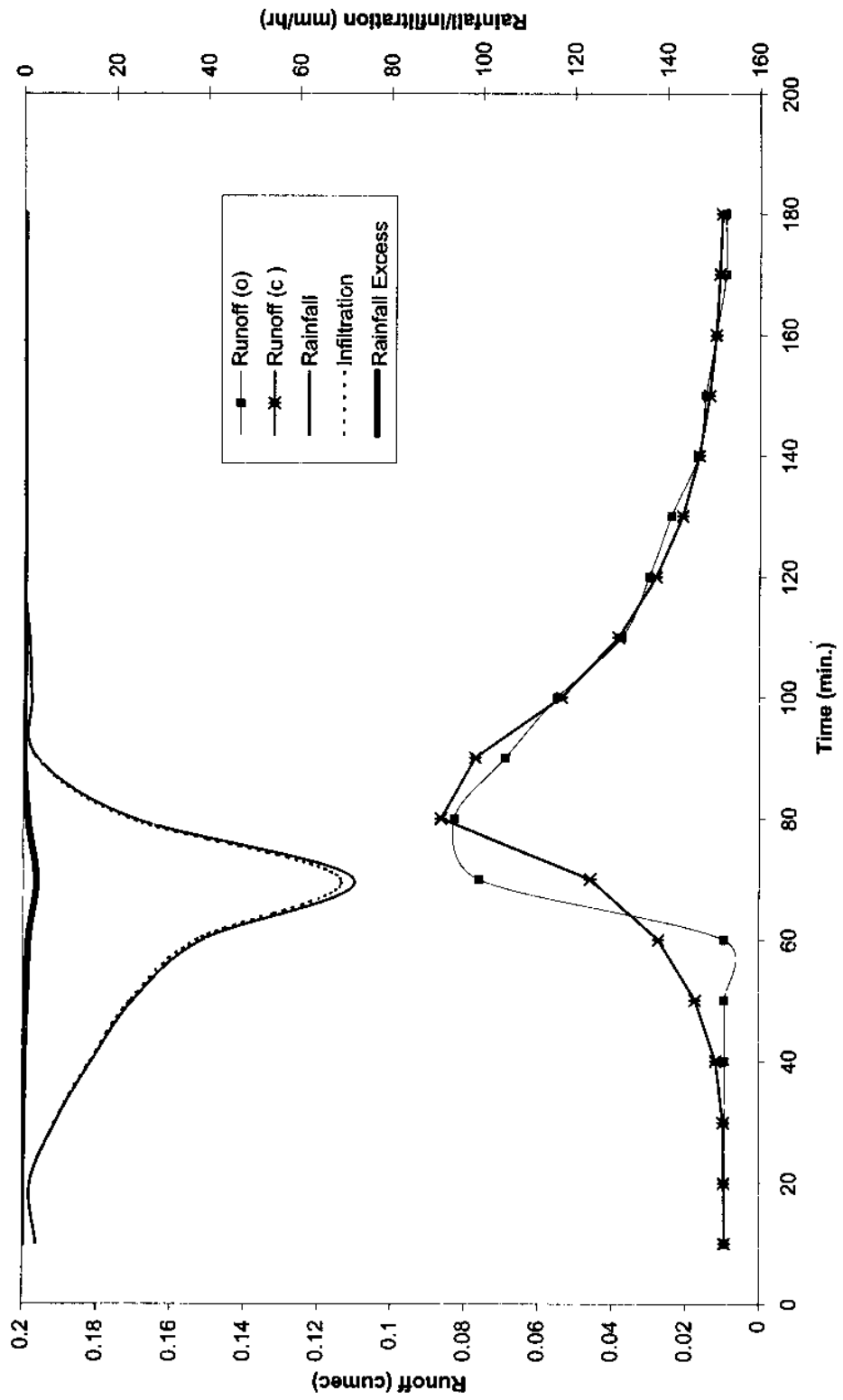


Fig. 8. Rainfall-runoff simulation of event 5 of Himalayan Jhandoo Nala watershed.

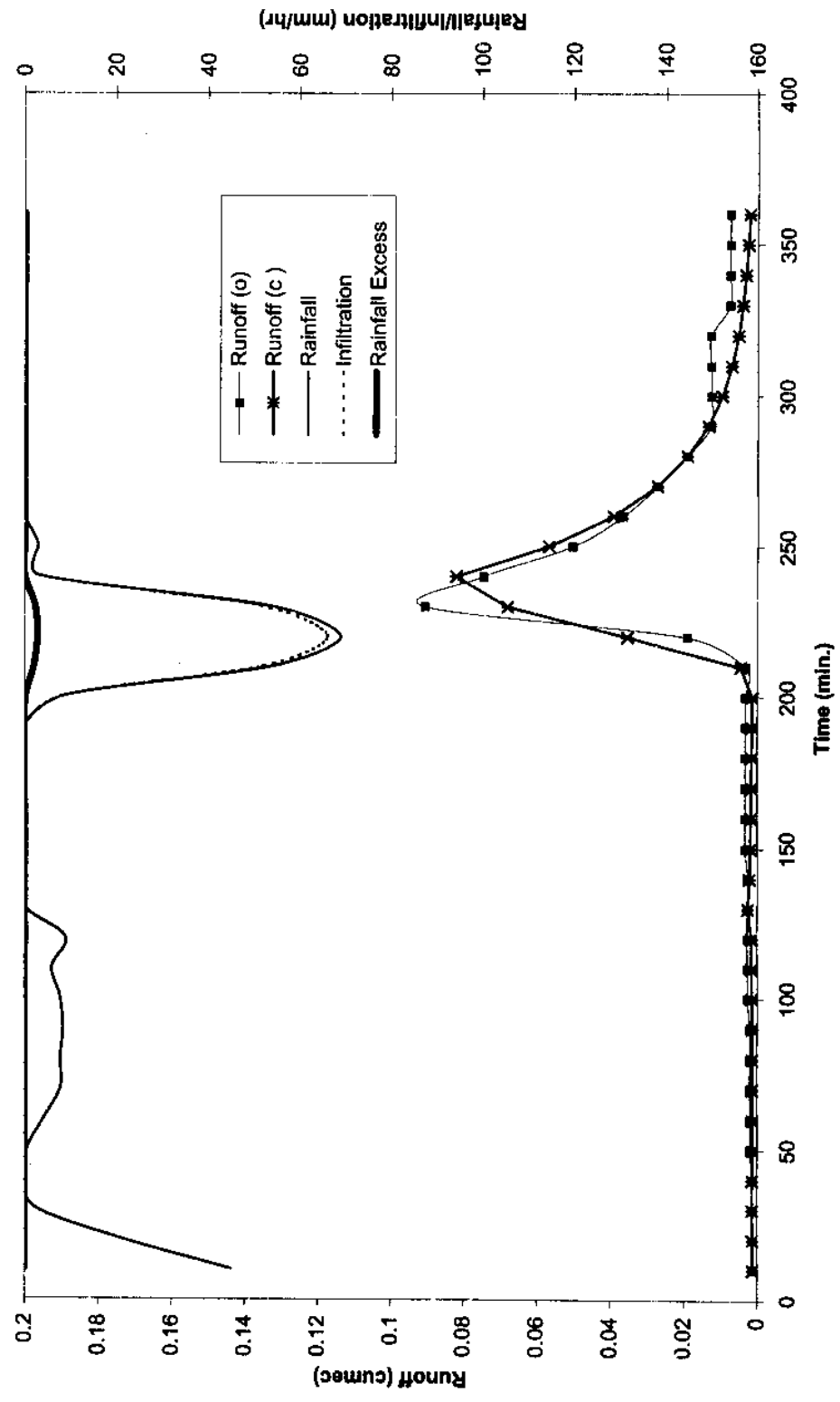


Fig. 9. Rainfall-runoff simulation of event 6 of Himalayan Jhandoo Nala watershed.

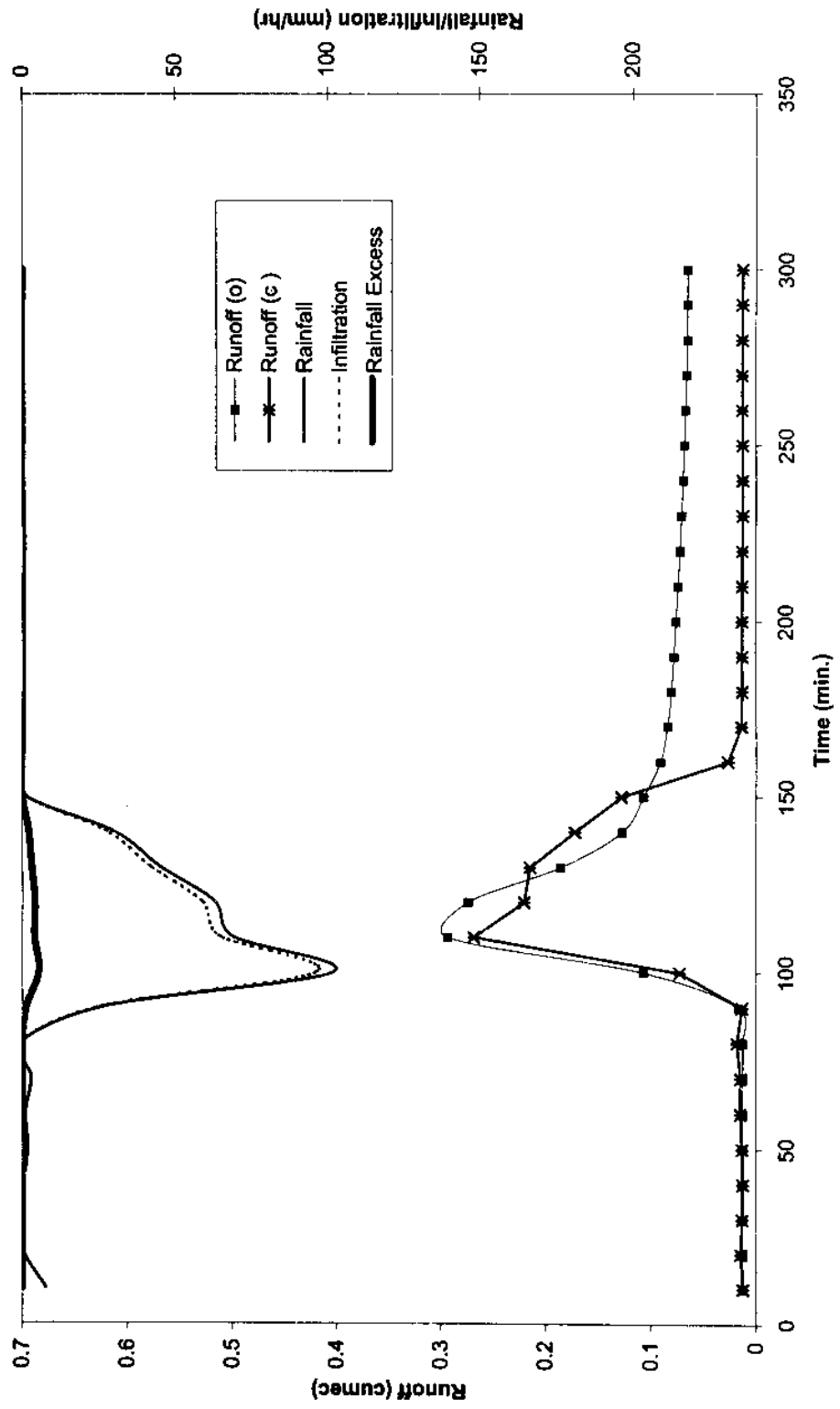


Fig. 10. Rainfall-runoff simulation of event 7 of Himalayan Jhandoo Nala watershed.

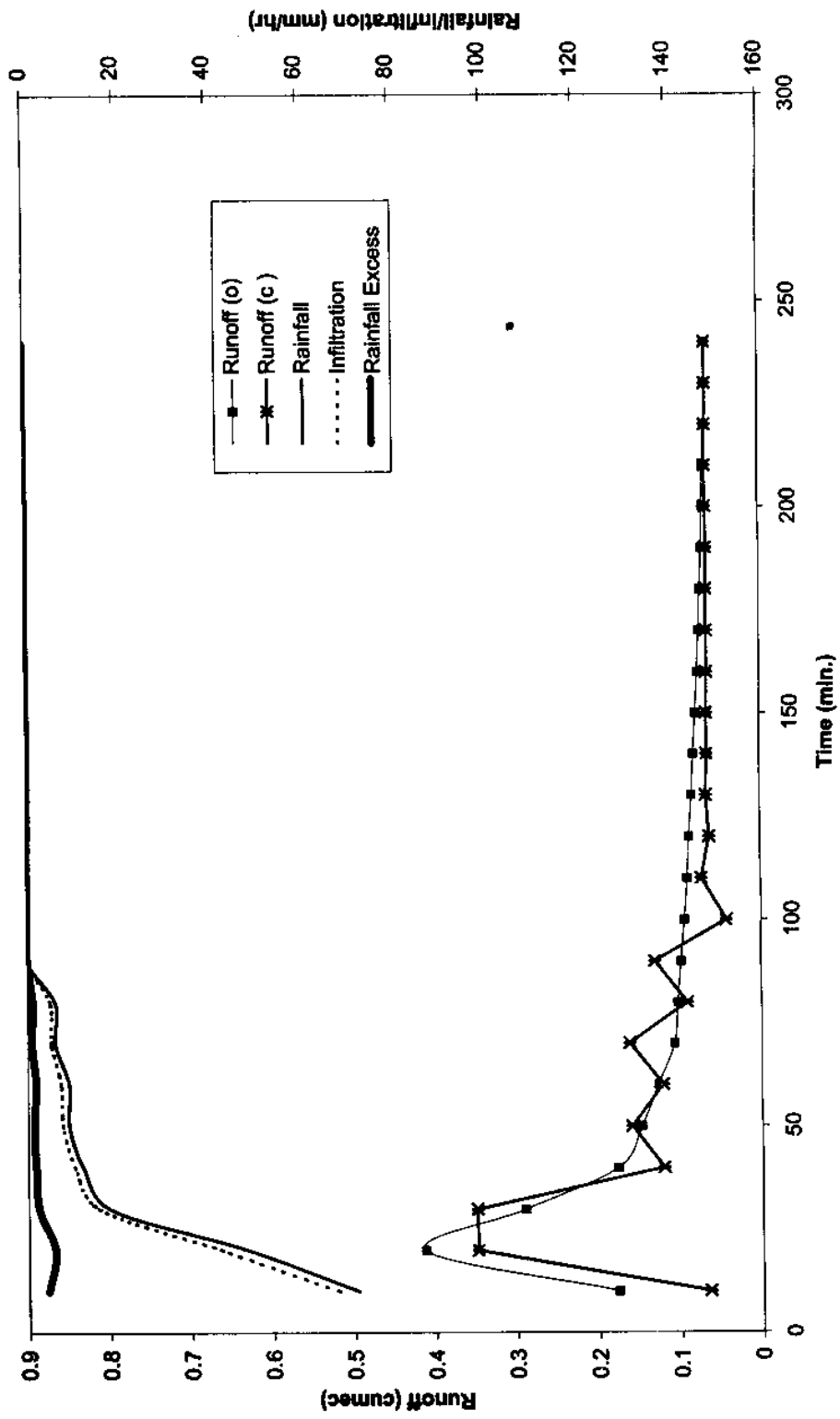




Fig. 11. Rainfall-runoff simulation of event 8 of Himalayan Jhandoo Nala watershed.

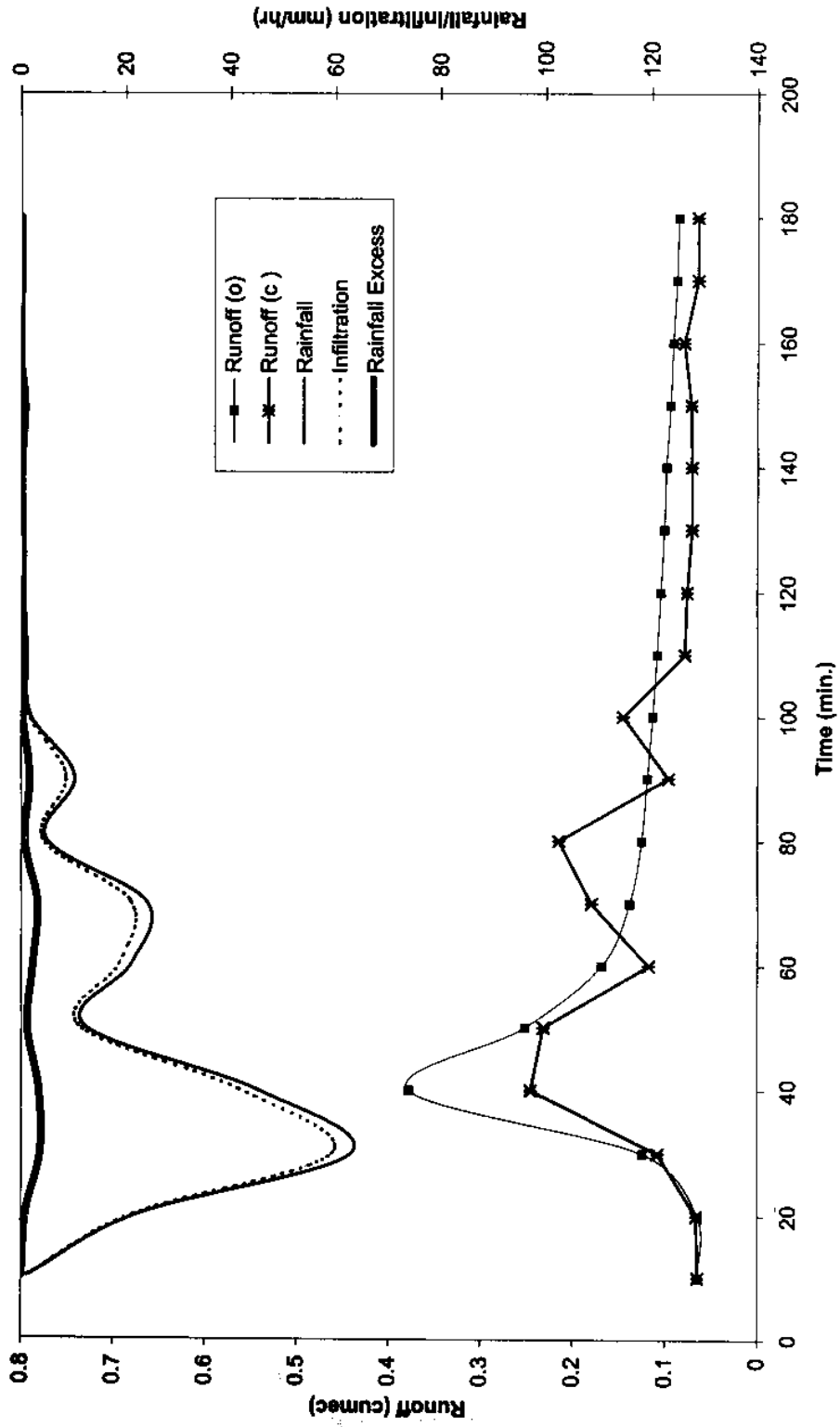


Fig. 12. Rainfall-runoff simulation of event 9 of Himalayan Jhandoo Nala watershed.

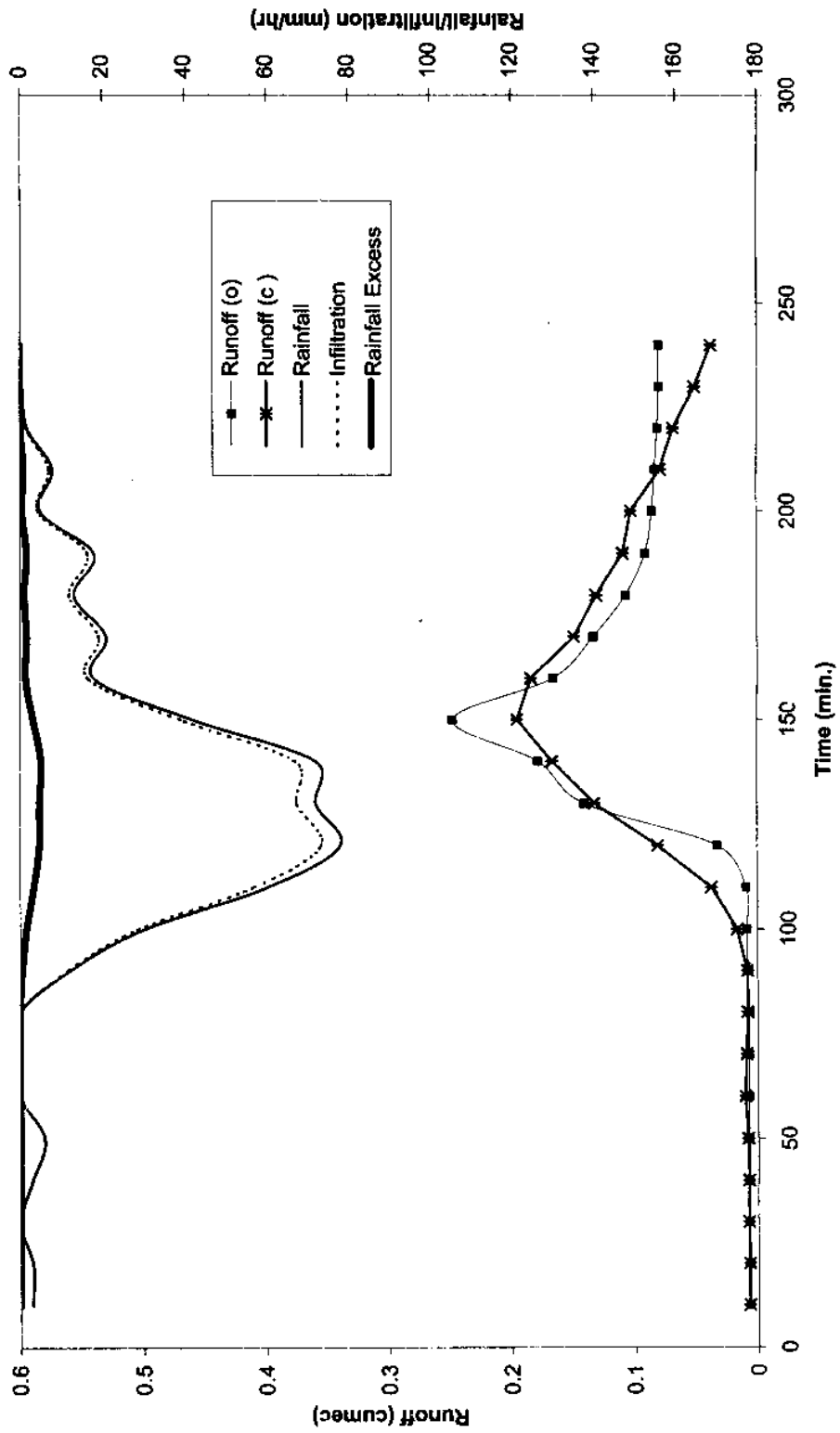


Fig. 13. Rainfall-runoff simulation of event 10 of Himalayan Jhandoo Nala watershed.

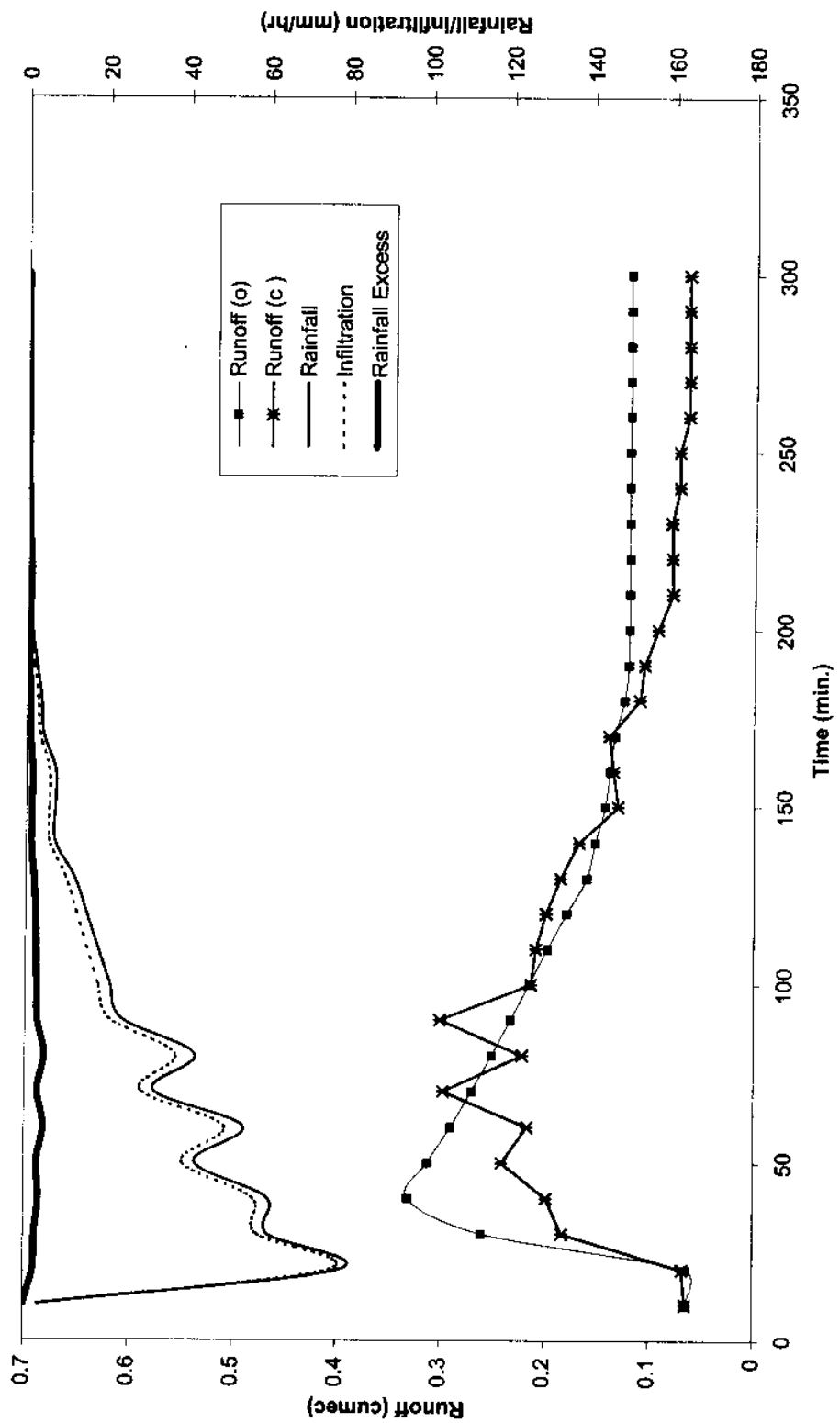


Fig. 14. Rainfall-runoff simulation of event 11 of Himalayan Jhandoo Nala watershed.

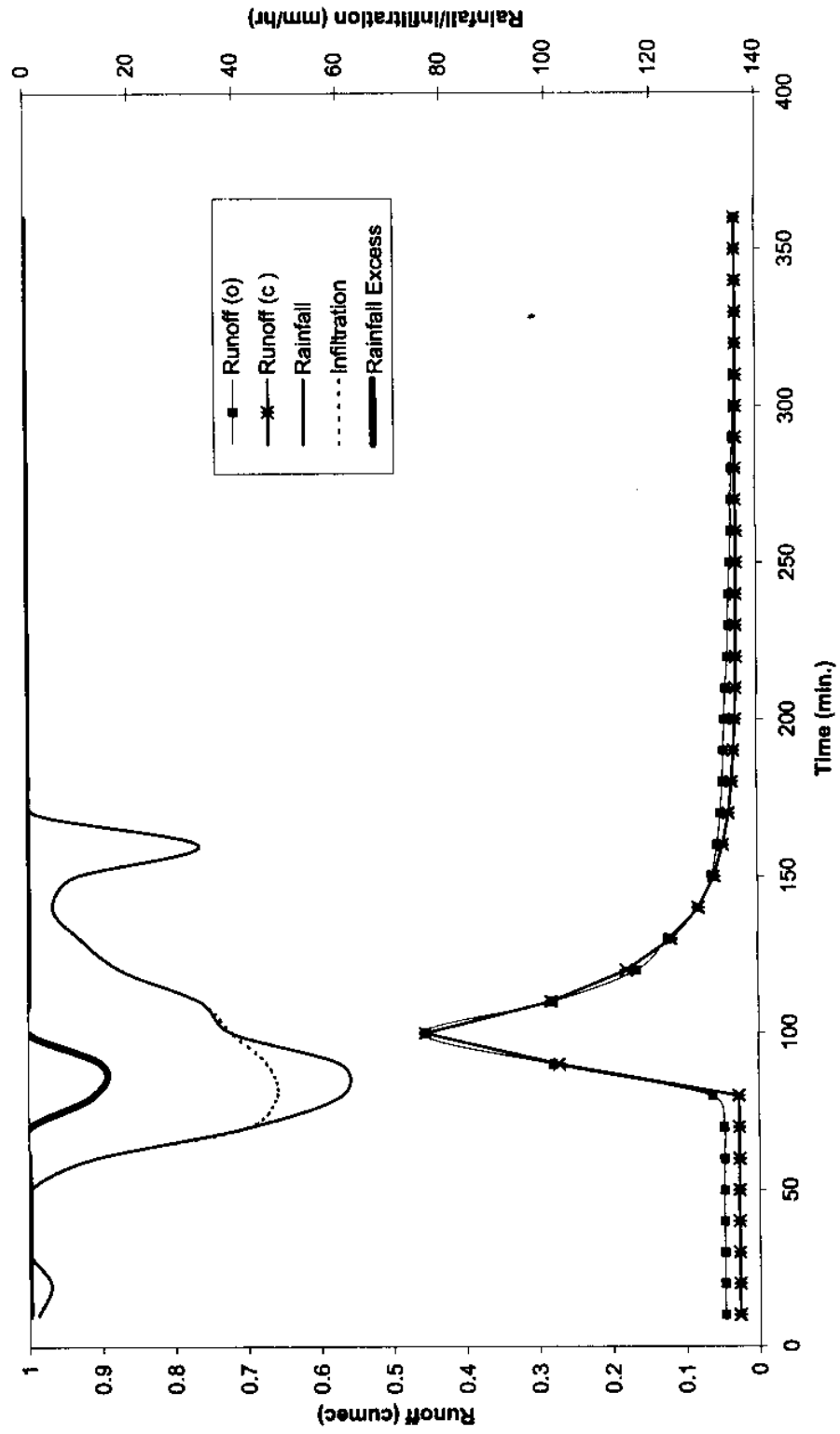


Fig. 15. Rainfall-runoff simulation of event 12 of Himalayan Jhandoo Nala watershed.

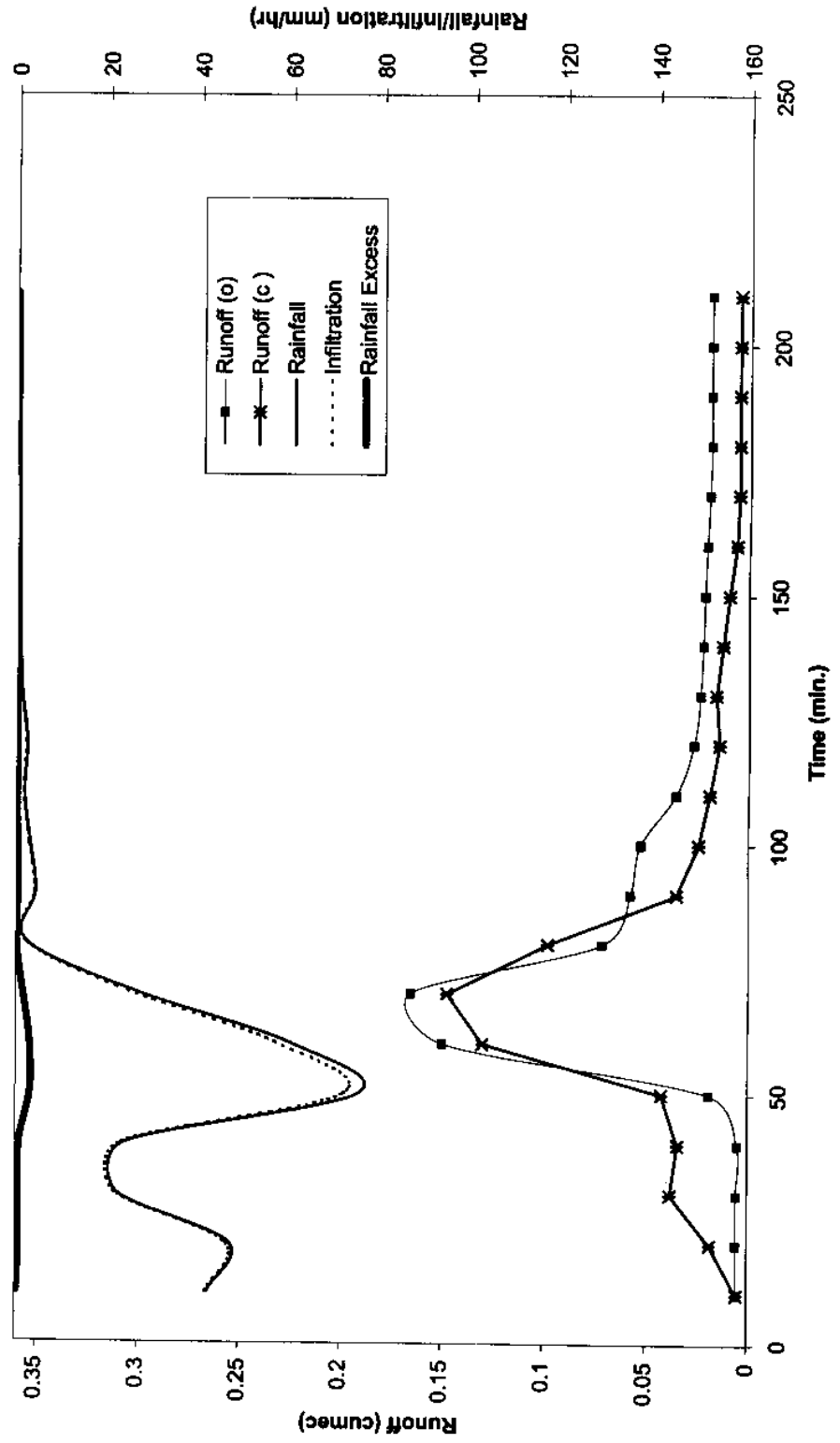


Fig. 16. Rainfall-runoff simulation of event 13 of Himalayan Jhandoo Nala watershed.

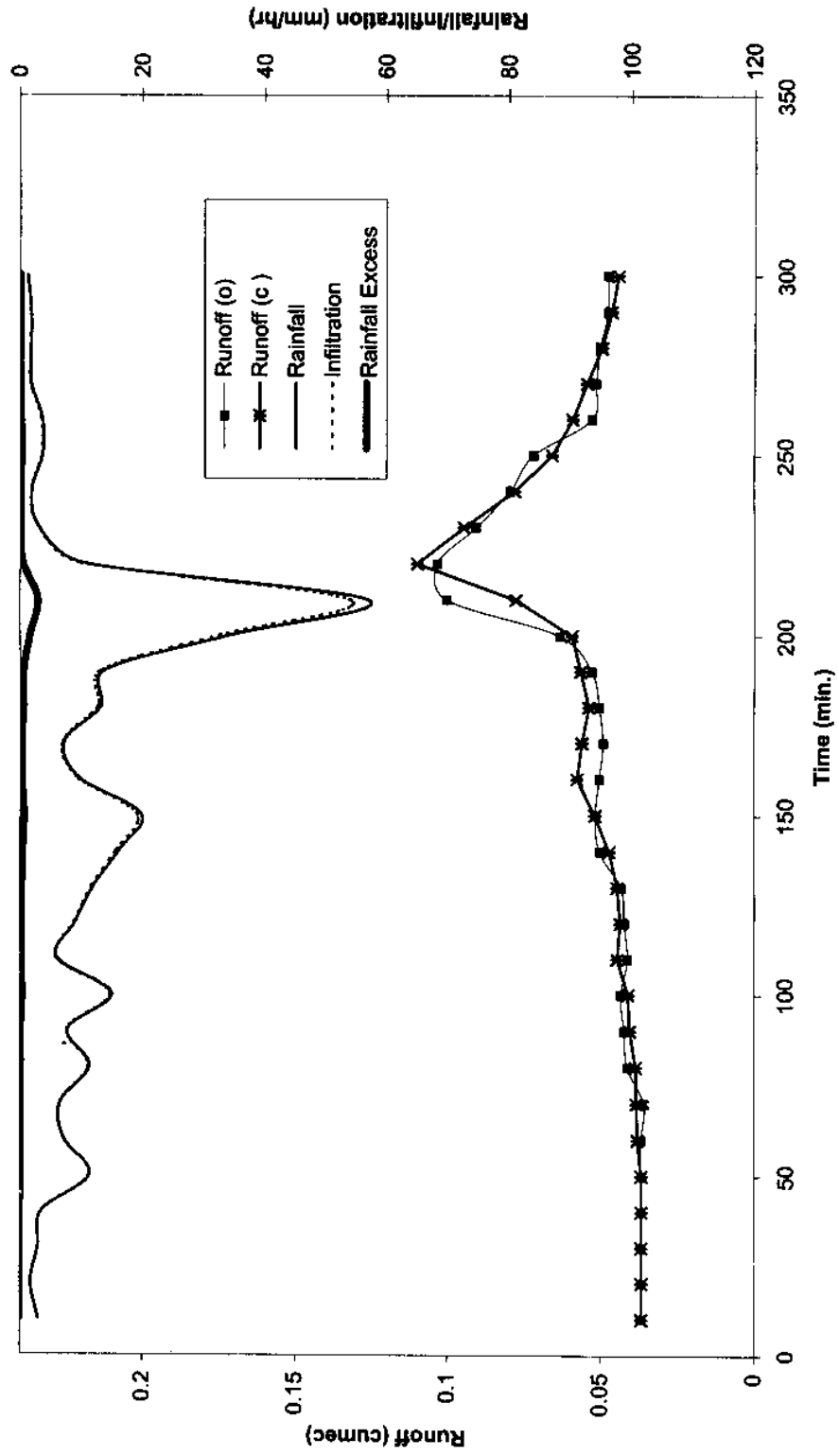


Fig. 17. Rainfall-runoff simulation of event 14 of Himalayan Jhandoo Nala watershed.

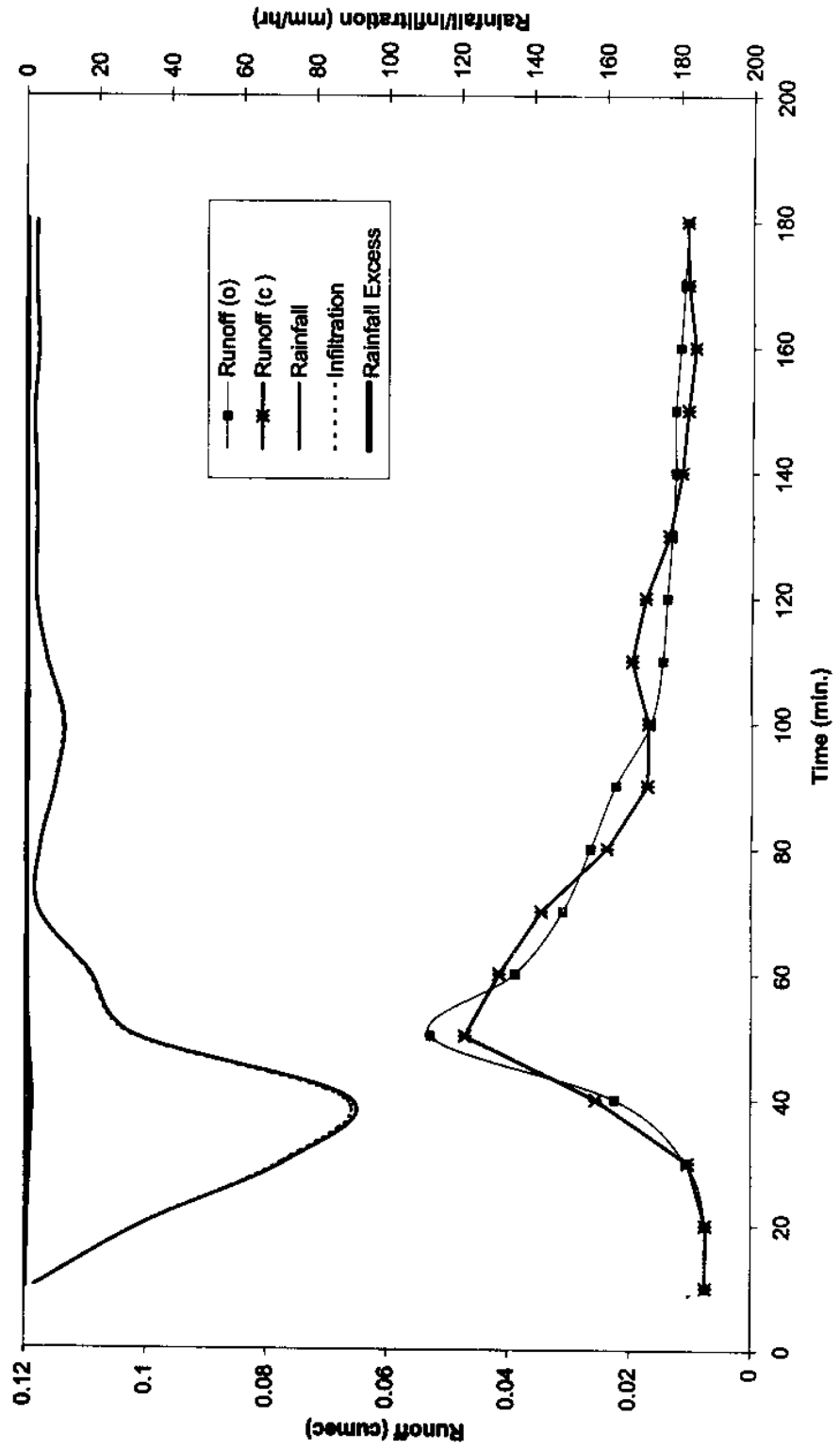


Fig. 18. Rainfall-runoff simulation of event 15 of Himalayan Jhandoo Nala watershed.

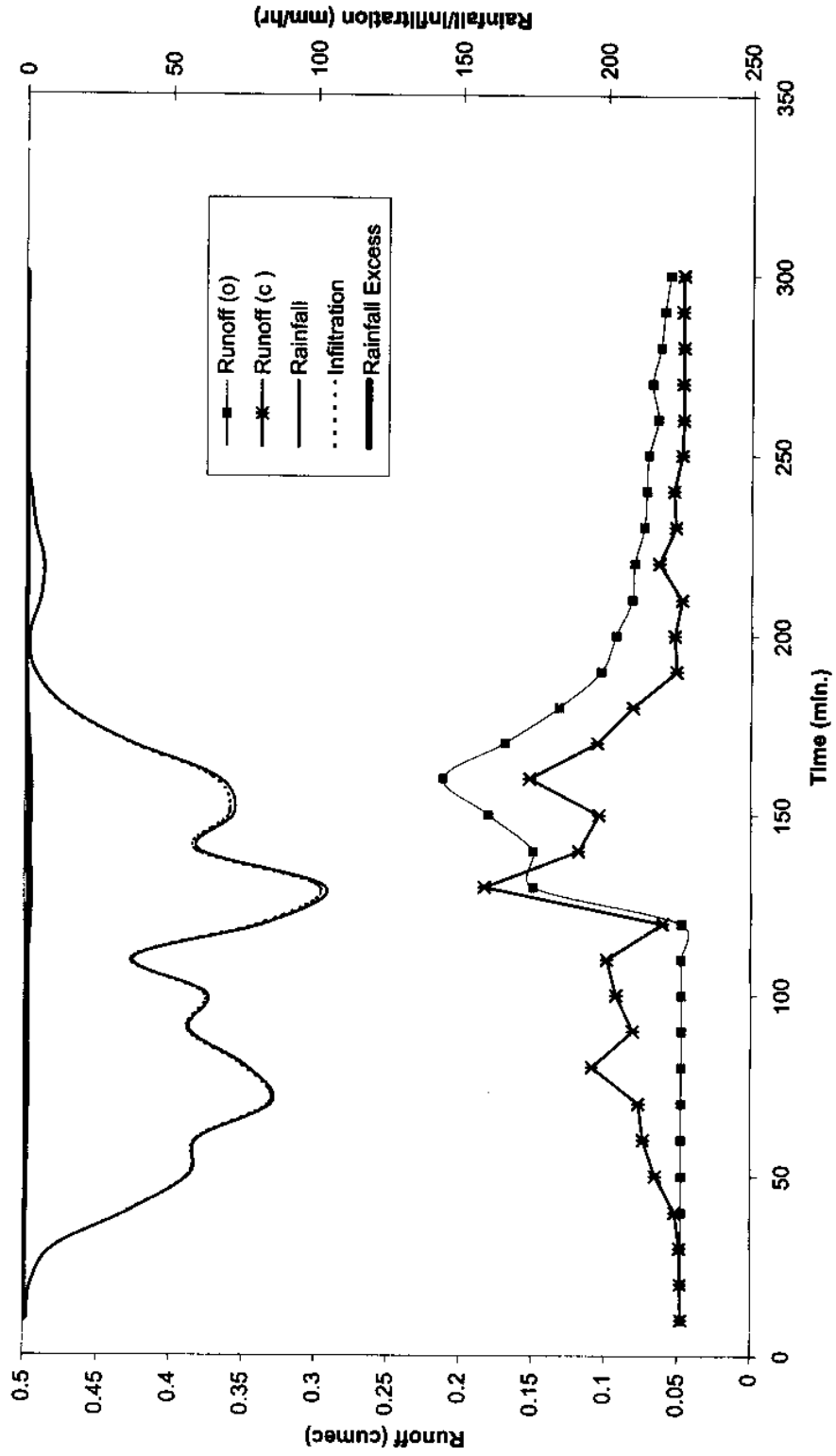




Fig. 19. Rainfall-runoff simulation of event 16 of Himalayan Jhandoo Nala watershed.

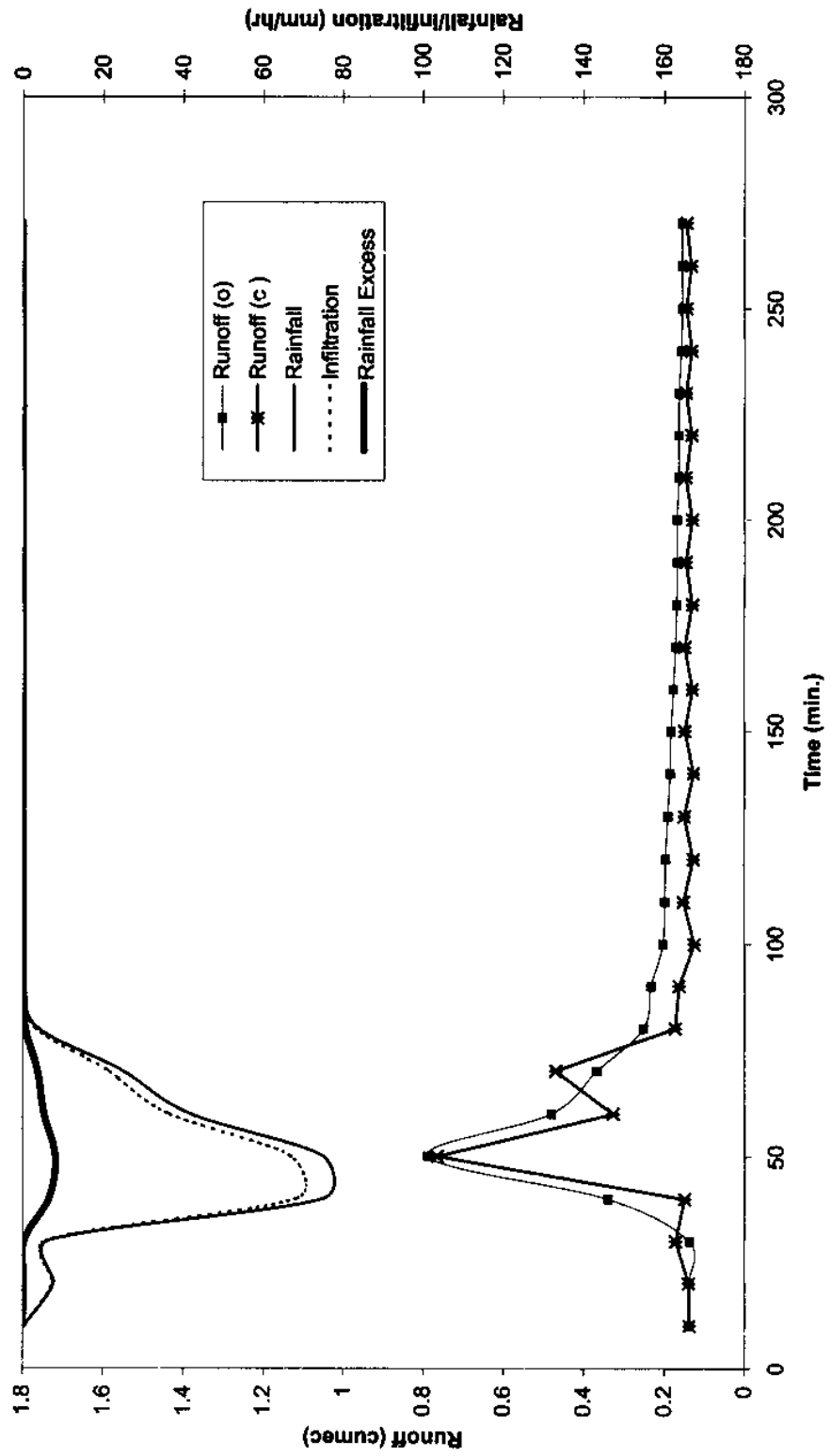


Fig. 20. Rainfall-runoff simulation of event 17 of Himalayan Jhandoo Nala watershed.

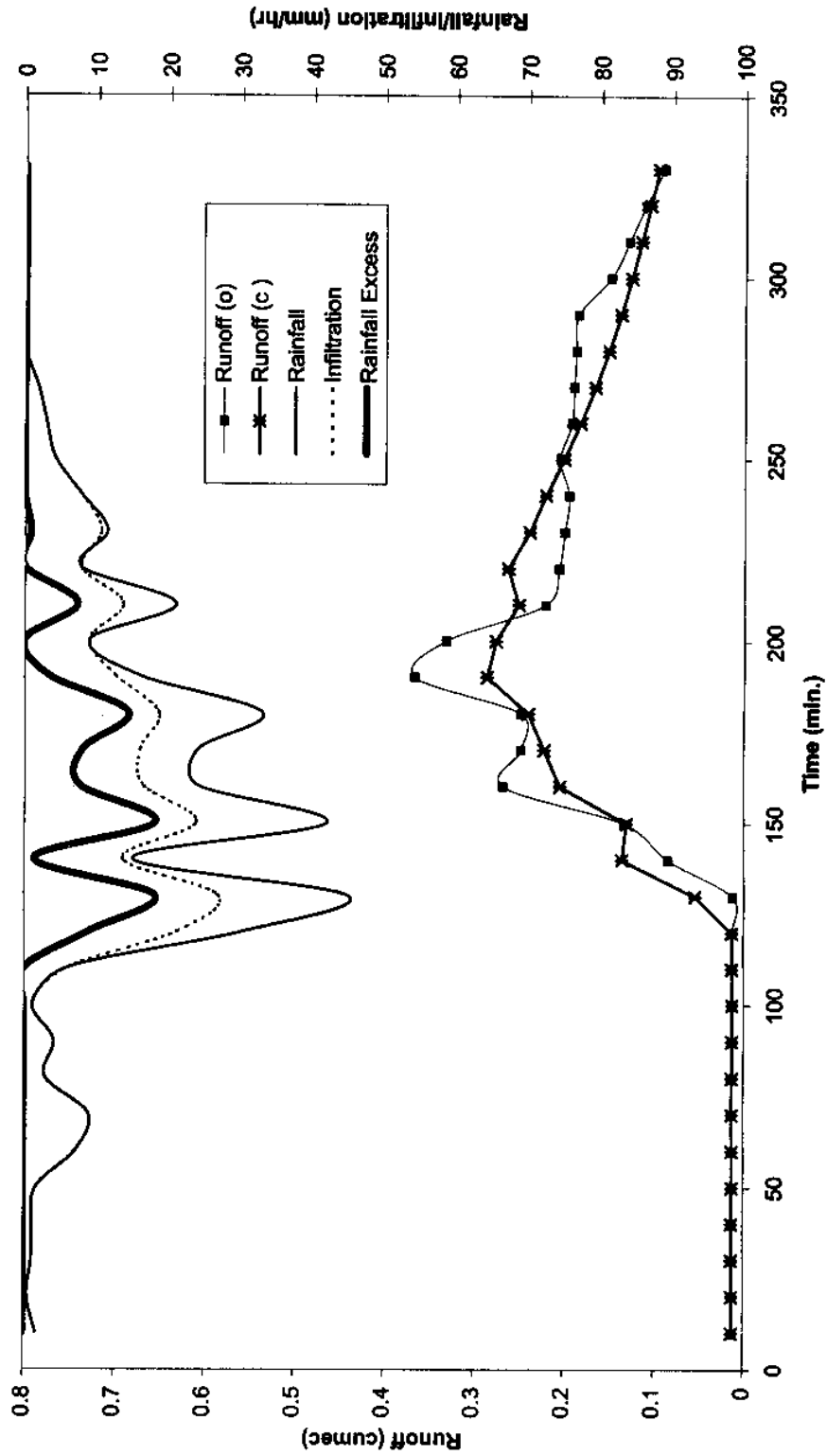


Fig. 21. Rainfall-runoff simulation of event 1 of Godavary basin.

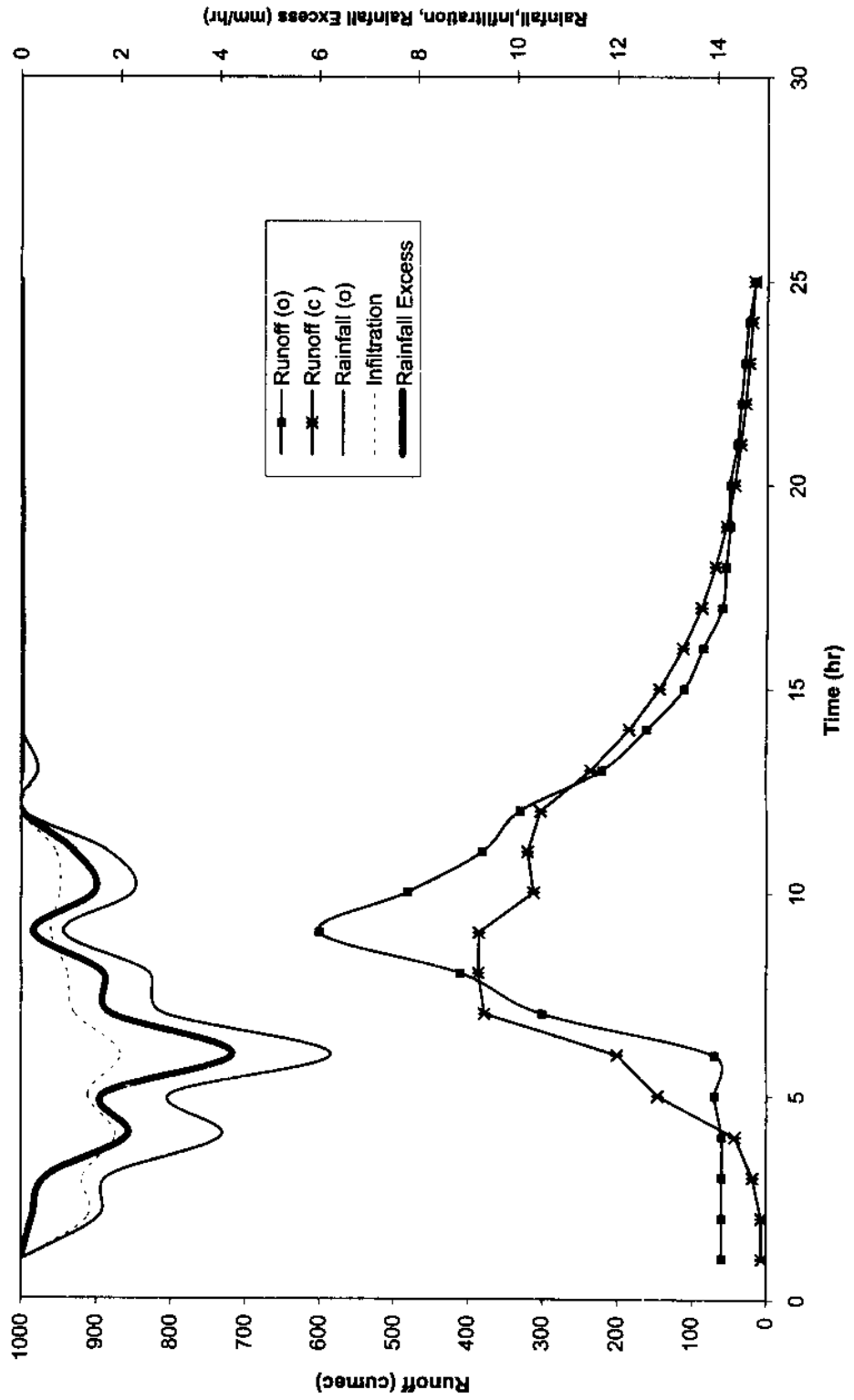


Fig. 22. Rainfall-runoff simulation of event 2 of Godavary basin.

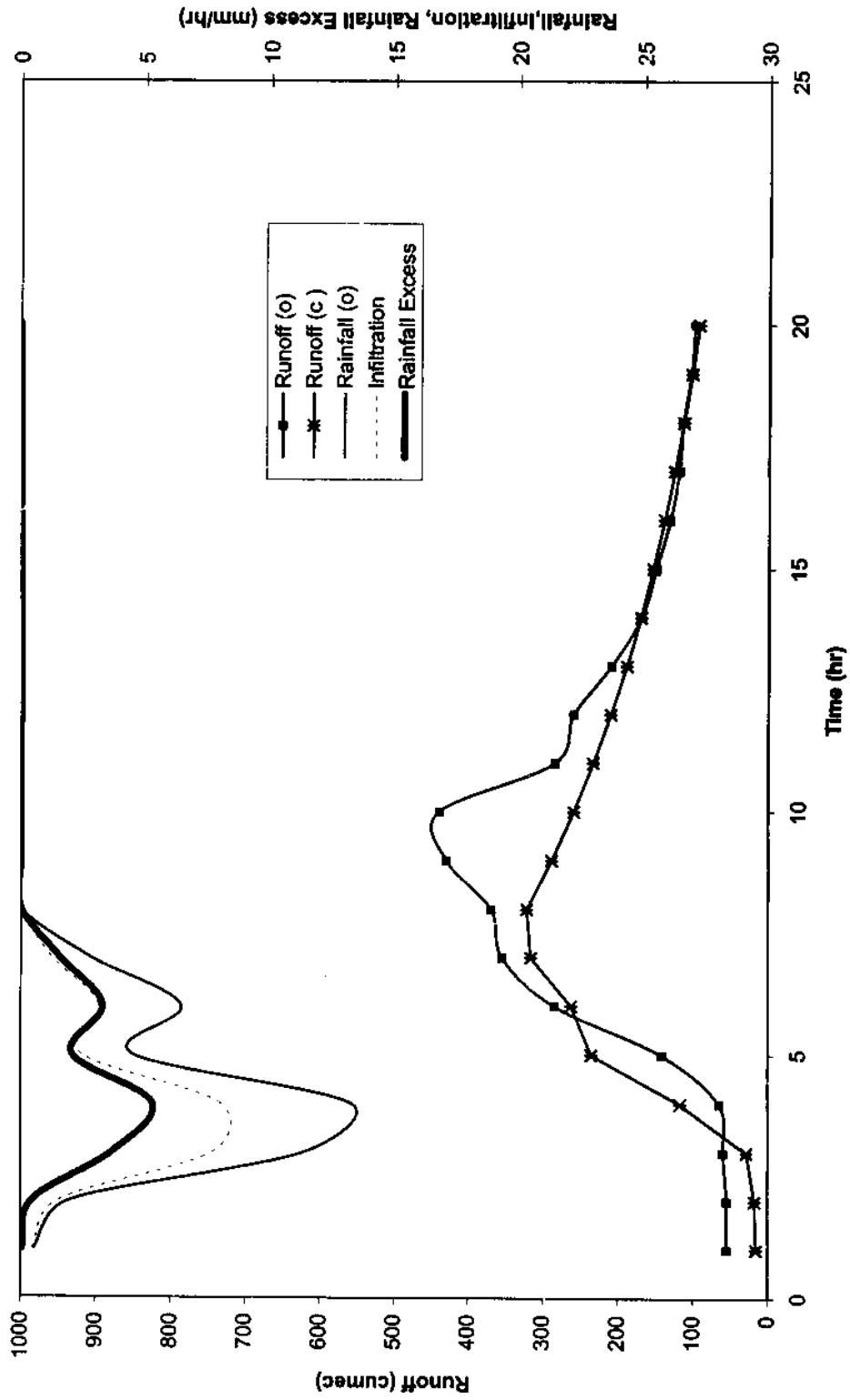


Fig. 23. Rainfall-runoff simulation of event 3 of Godavary basin.

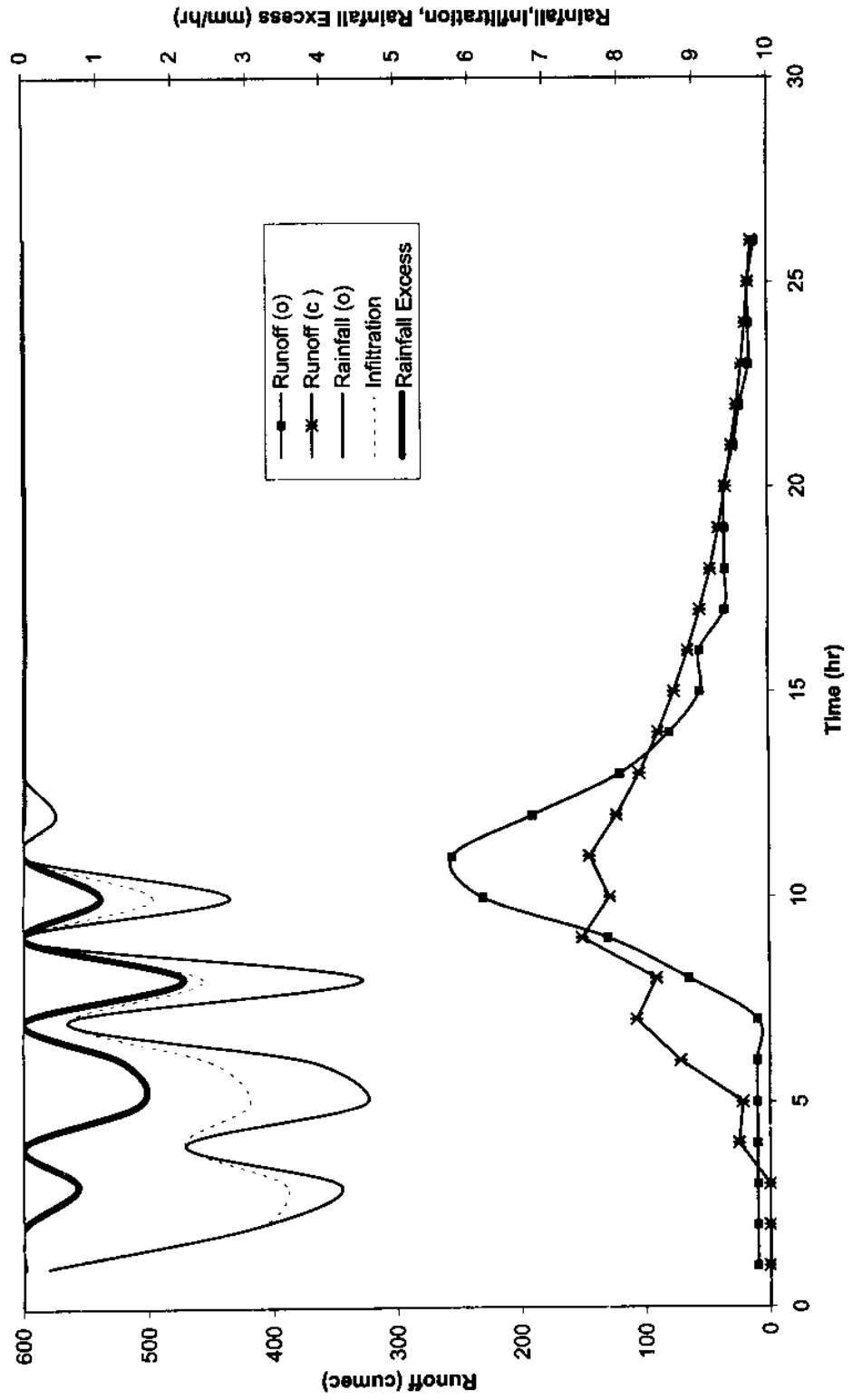


Fig. 24. Rainfall-runoff simulation of event 4 of Godavary basin.

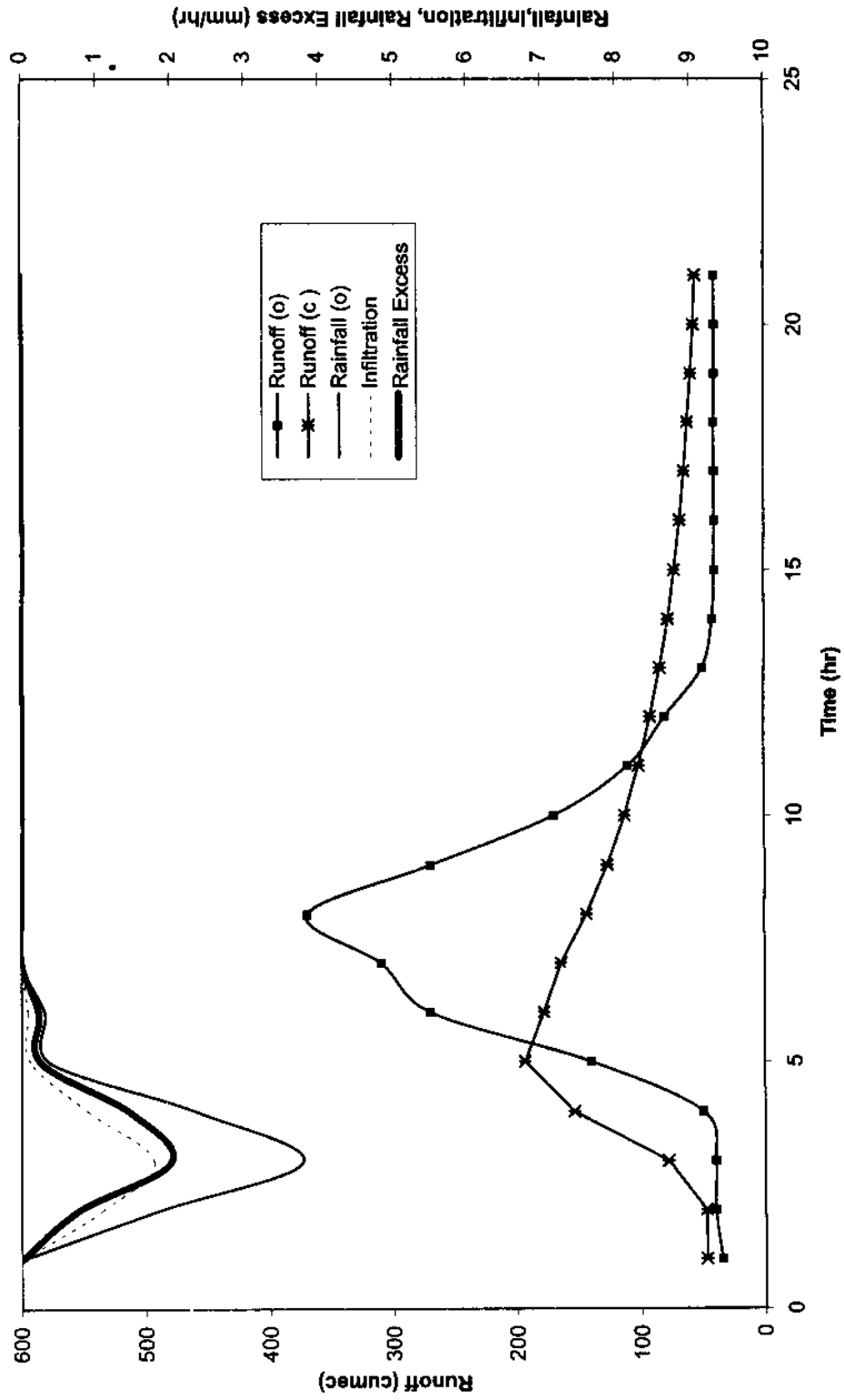


Fig. 25. Rainfall-runoff simulation of event 5 of Godavary basin.

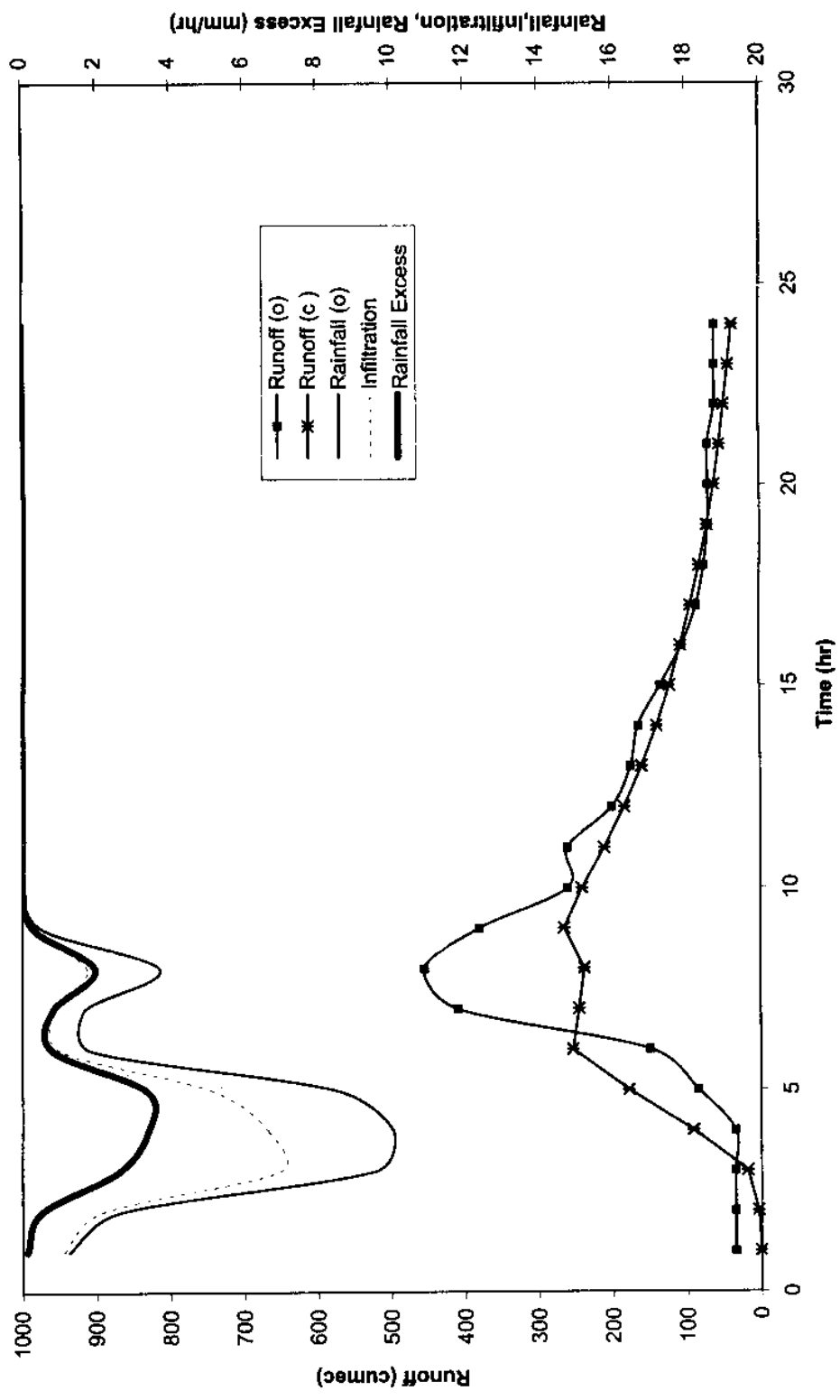


Fig. 26. Rainfall-runoff simulation of event 6 of Godavary basin.

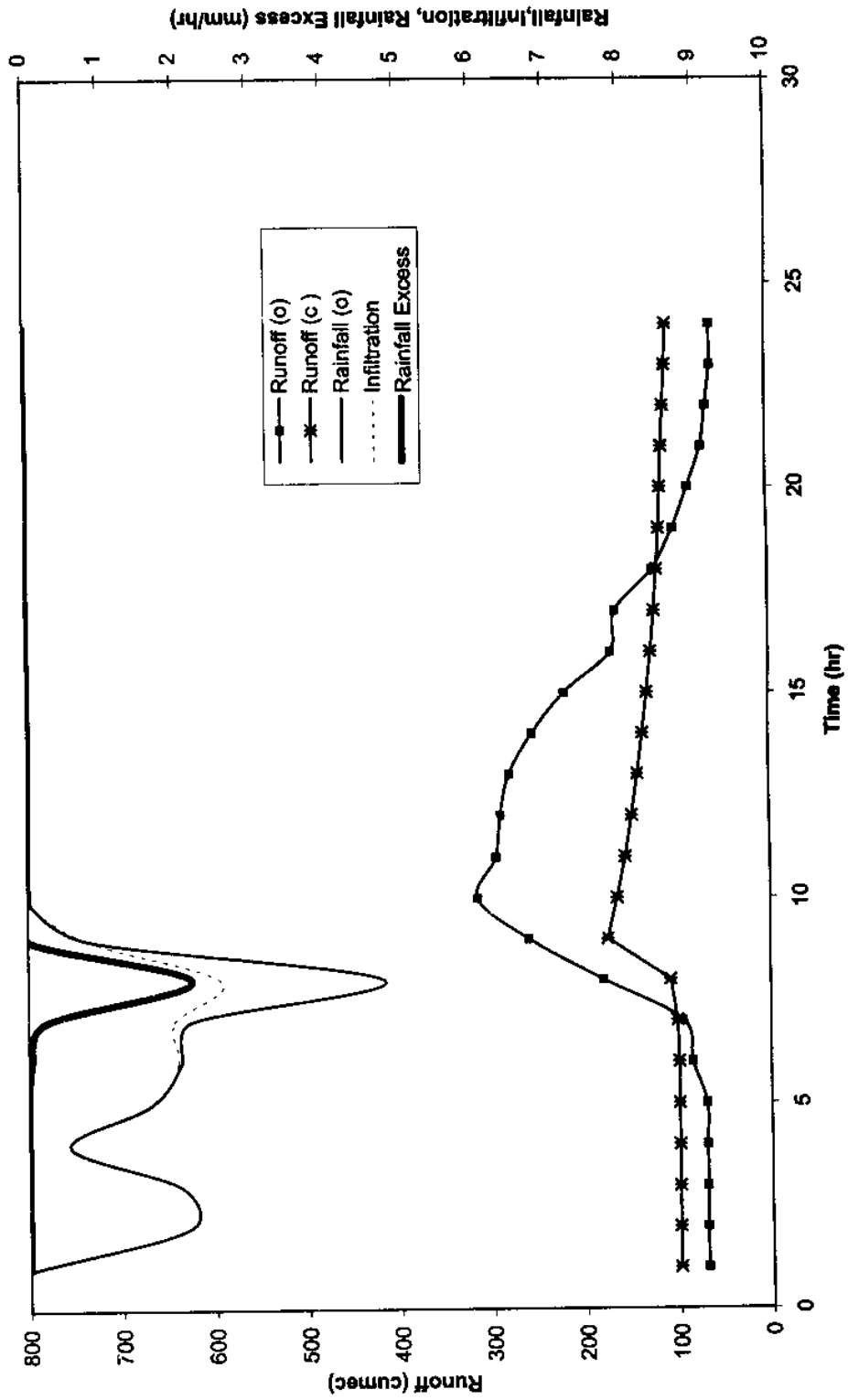
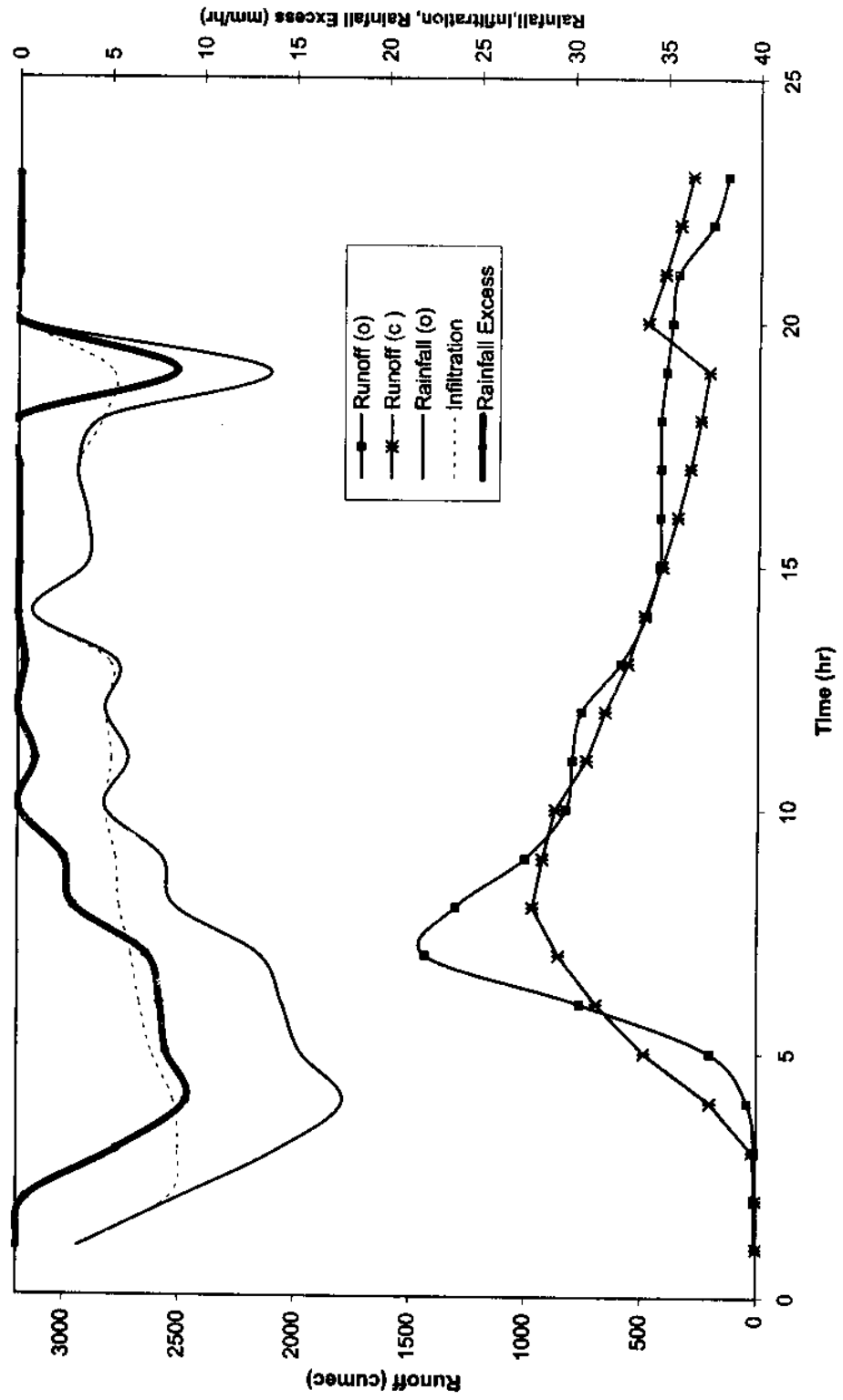




Fig. 27. Rainfall-runoff simulation of event 7 of Godavary basin.



$$r^2 = 1 - \frac{\sum_{l=1}^N (Q_o - Q_c)_l^2}{\sum_{l=1}^N (Q_o - Q_m)_l^2} \quad (47)$$

where N is the number of ordinates in an event, l is an integer varying from 1 to N, m is the number of model parameters (=3 for the events of Jhandoo Nala watershed and 4 for the 3F sub-zone watershed of Godavary),  $Q_o$  is the observed discharge,  $Q_c$  is the computed discharge, and  $Q_m$  is the mean discharge. The higher values of SE and lower values of  $r^2$  show a poor fit whereas the lower values of SE and the higher values of  $r^2$  show that the model fits well. The value of  $r^2$  varies on the scale of 0-1; 0 indicates that a mean model fits better than the model proposed and 1 exhibits a perfect fit.

#### d) Computation of Model Parameters and Simulation Results

The computed model parameters the infiltration decay coefficient 'k', storage coefficient K, and minimum infiltration rate  $f_c$  range respectively from  $7.83 \cdot 10^{-5}$  to  $1.02 \cdot 10^{-2} \text{ min}^{-1}$ , from 0.13 to 99.40 min, and from 0.0 to 1.45 cumec. Similarly, from Table 2 and the corresponding Figs. 21 through 27 it is visible that the peak discharges of the events vary from 255 to 1432 cumecs, time to peak from 8 to 11 hrs, baseflow from 0 to 47.34 cumecs, and the time base ranges between 20 and 26 hrs. The computed model parameters the infiltration decay coefficient 'k', storage coefficient K, and minimum infiltration rate  $f_c$  range respectively from 0.0573 to 0.2920  $\text{hr}^{-1}$ , from 3.89 to 8.82 hrs, and from 0 to 1080 cumec. It is worth noting that the baseflow for the events of Table 2 was also optimised along with the above parameters. These parameters (Table 1) are computed with standard error varying from 0.0031 to 0.0681 and  $r^2$  varying from 0.3975 to 0.9782. Out of 17 events, 13 events are simulated with  $r^2$  greater than 0.70, exhibiting a reasonably good performance of the model. Similarly, from Table 2 it is apparent that 3 events yield  $r^2 > 0.7$  and 5 events yield  $r^2 > 0.6$ , showing reasonably good performance. It is also visible from Tables 1 and 2 and Figs. 4 through 27 that the values of peak discharge and time to peak discharges also, in general, fairly well. To show the model

performance a volumetric analysis of simulation results is also performed, in what follows.

Table 3 shows the volumetric analysis for the events of Jhandoo Nala watershed. It is apparent that infiltration forms a major component of rainfall-runoff simulation. This is due to the soil of the watershed being highly porous because of dynamic explosions for mining of lime stone, as indicated above. The direct runoff is computed subtracting the baseflow from the total runoff. The deviation of the computed values of direct runoff, total runoff, and mass balance from the observed ones is shown using relative error:

$$\text{Relative error (\%)} = (\text{observed} - \text{computed}) * 100 / \text{observed} \quad (48)$$

The higher value of the relative error is indicative of greater deviation and vice versa. Its 0 value indicates a perfect fit.

Computation of infiltration, direct runoff, and mass balance of Tables 3 and 4 is exemplified through Tables 5 and 6, respectively, for the event 3 of Jhandoo Nala watershed and 3F sub-zone watershed of Godavary. It is apparent from Table 3 that the values of relative errors for direct runoff range between -40.18 and 46.47%. Similarly, the relative errors for total runoff computation range between -63.29 and 16.96% and error in mass conservation range between -4.30 and 4.86%. It indicates that the total runoff is simulated better than the direct runoff and the mass is conserved well in the model simulation. Similarly, in the simulation of events of Godavary (Table 4), the direct runoff and total runoff are simulated with the relative errors ranging from 0.42 to 65.02% and from 0.42 to 17.85%, respectively. The mass is conserved with the errors ranging from 0.56 to 7.00%, which is within the reasonable limit of tolerance. These errors are, however, due to linear interpolation of the discharge ordinates in volume computation. It is worth mentioning that relative errors may range from 0 to  $\infty$  depending on the extent of fit and the amount of the observed variable. If the observed variable approaches zero, the relative error approaches infinity. Thus, these errors are indicative of the model

TABLE 3. VOLUMETRIC STATISTICS OF THE RAINFALL-RUNOFF EVENTS OF JHANDOO NALA WATERSHED

Event	Rainfall	Infiltration	Baseflow	Direct runoff (o)		Direct runoff (c)	Rel. error in direct runoff		Total runoff (o)		Total runoff (c)	Rel. error in total runoff		Error in mass conservation
	mm	mm	mm	mm	mm	mm	%	%	mm	mm	mm	%	%	%
1	49.53	48.01	2.33	1.67	1.53	8.36	4.00	3.85	-3.87	-0.02				
2	34.50	33.58	1.66	1.72	2.41	-40.18	3.38	4.07	16.96	-4.30				
3	45.50	42.96	2.77	2.83	2.54	10.29	5.59	5.30	-5.49	0.01				
4	32.00	30.88	0.57	1.09	1.11	-1.83	1.67	1.69	1.18	0.01				
5	52.00	50.76	0.16	1.37	1.23	9.81	1.53	1.39	-9.64	0.01				
6	58.70	55.22	1.29	6.49	3.48	46.47	7.79	4.77	-63.29	0.00				
7	30.00	26.80	5.26	4.13	3.28	20.47	9.39	8.46	-11.01	-0.29				
8	34.90	31.92	3.95	3.90	2.98	23.75	7.85	6.92	-13.41	0.00				
9	77.70	72.61	0.59	4.79	4.88	-1.70	5.39	5.47	1.49	0.27				
10	83.00	75.38	6.58	10.27	7.62	25.83	16.85	14.19	-18.69	0.00				
11	54.90	50.48	3.32	5.53	4.42	20.04	8.85	7.74	-14.32	0.00				
12	52.00	50.07	0.37	2.30	1.93	15.97	2.67	2.30	-15.95	0.00				
13	49.60	47.94	3.73	1.60	1.60	0.02	5.33	5.33	0.06	0.12				
14	50.00	49.31	0.09	0.00	0.00	0.00	0.09	0.09	0.00	1.38				
15	157.30	154.67	4.85	3.49	2.64	24.40	8.34	7.48	-11.40	0.00				
16	39.20	34.99	12.66	7.66	4.50	41.25	20.31	16.88	-20.34	-0.72				
17	55.40	40.70	1.42	12.51	12.00	4.05	13.93	13.42	-3.78	4.86				

**TABLE 4. VOLUMETRIC STATISTICS OF THE RAINFALL-RUNOFF EVENTS OF 3FSUB-ZONE WATERSHED OF GODAVARY**

Event	Rainfall (o)		Infiltration		Baseflow		Direct runoff (o)		Direct runoff (c)		Rel. error in direct runoff		Total runoff (o)		Total runoff (c)		Rel. error in total runoff		Error in mass conservation	
	mm		mm		mm		mm		mm		%		mm		mm		%		%	
1	27.23		12.27		0.73		15.95		14.80		7.18		16.68		15.53		6.87			0.56
2	40.85		24.50		1.36		15.70		13.50		14.04		17.06		14.86		12.92			7.00
3	26.64		19.82		0.00		6.53		6.50		0.42		6.53		6.50		0.42			1.20
4	8.67		3.97		4.34		5.89		4.55		22.73		9.87		8.89		9.87			1.78
5	39.83		25.88		0.00		15.17		12.87		15.17		15.17		12.87		15.17			2.72
6	16.24		13.76		10.43		6.40		2.24		65.02		15.42		12.67		17.85			1.47
7	153.42		100.29		0.00		49.79		45.96		7.70		49.79		45.96		7.70			4.67

**TABLE 5. AN EXAMPLE APPLICATION OF THE MODEL FOR EVENT 3 OF JHANDOO NALA WATERSHED**

Time	Rainfall	Infiltration	Baseflow	Observed		Computed	
				Total runoff	Direct runoff	Total runoff	Direct runoff
min	mm/hr	mm/hr	cumec	cumec	cumec	cumec	cumec
10	1.8	1.8000	0.0272	0.0272	0.0000	0.0272	0.0000
20	4.2	4.2000	0.0272	0.0272	0.0000	0.0272	0.0000
30	12.0	12.0000	0.0272	0.0272	0.0000	0.0272	0.0000
40	15.0	14.9654	0.0272	0.0272	0.0000	0.0272	0.0000
50	3.0	3.0000	0.0272	0.0272	0.0000	0.0278	0.0006
60	4.2	4.2000	0.0272	0.0272	0.0000	0.0276	0.0004
70	4.8	4.8000	0.0272	0.0272	0.0000	0.0275	0.0003
80	9.0	8.8917	0.0272	0.0272	0.0000	0.0274	0.0002
90	24.0	22.9098	0.0272	0.0300	0.0028	0.0292	0.0020
100	6.0	5.9784	0.0272	0.0455	0.0183	0.0481	0.0209
110	12.0	11.4933	0.0272	0.0319	0.0047	0.0408	0.0136
120	27.0	25.2055	0.0272	0.0389	0.0117	0.0450	0.0178
130	54.0	49.6852	0.0272	0.0690	0.0418	0.0707	0.0435
140	39.0	35.7485	0.0272	0.1760	0.1488	0.1323	0.1051
150	12.0	11.1932	0.0272	0.1230	0.0958	0.1523	0.1251
160	6.0	5.7532	0.0272	0.1230	0.0958	0.1211	0.0939
170	12.0	11.0476	0.0272	0.0805	0.0533	0.0912	0.0640
180	15.0	13.6233	0.0272	0.0805	0.0533	0.0849	0.0577
190	9.0	8.2753	0.0272	0.0782	0.0510	0.0886	0.0614
200	3.0	2.9985	0.0272	0.0747	0.0475	0.0792	0.0520
210	0.0	0.0000	0.0272	0.0690	0.0418	0.0602	0.0330
220	0.0	0.0000	0.0272	0.0605	0.0333	0.0482	0.0210
230	0.0	0.0000	0.0272	0.0605	0.0333	0.0405	0.0133
240	0.0	0.0000	0.0272	0.0528	0.0256	0.0356	0.0084
250	0.0	0.0000	0.0272	0.0477	0.0205	0.0326	0.0054
260	0.0	0.0000	0.0272	0.0433	0.0161	0.0306	0.0034
270	0.0	0.0000	0.0272	0.0400	0.0128	0.0294	0.0022
280	0.0	0.0000	0.0272	0.0378	0.0106	0.0286	0.0014
290	0.0	0.0000	0.0272	0.0357	0.0085	0.0281	0.0009
300	0.0	0.0000	0.0272	0.0338	0.0066	0.0278	0.0006
Sum (ordinates)	273.0	257.7689	0.8160	1.6499	0.8339	1.5641	0.7481
Volume (mm)	45.5	42.9615	2.7661	5.5929	2.8268	5.3020	2.5359

**TABLE 6. AN EXAMPLE APPLICATION OF THE SCS-CN BASED MODEL FOR EVENT 1 OF 3F SUB-ZONE WATERSHED OF GODAVARY**

Time	Rainfall	Infiltration	Baseflow	Observed		Computed	
				Total runoff	Direct runoff	Total Runoff	Direct runoff
hr	mm/hr	mm/hr	cumec	cumec	cumec	cumec	cumec
1	0.09	0.09	6.64	60.00	53.36	6.64	0.00
2	1.56	1.34	6.64	60.00	53.36	6.64	0.00
3	1.75	1.24	6.64	60.00	53.36	18.26	11.62
4	4.03	1.89	6.64	60.00	53.36	42.44	35.80
5	2.99	1.34	6.64	70.00	63.36	145.72	139.08
6	6.24	1.99	6.64	70.00	63.36	200.05	193.41
7	2.83	1.06	6.64	300.00	293.36	377.47	370.83
8	2.56	0.93	6.64	410.00	403.36	385.37	378.73
9	0.85	0.60	6.64	600.00	593.36	384.17	377.53
10	2.27	0.78	6.64	480.00	473.36	311.02	304.38
11	1.72	0.68	6.64	380.00	373.36	319.33	312.69
12	0.00	0.00	6.64	330.00	323.36	302.39	295.75
13	0.34	0.34	6.64	220.00	213.36	234.98	228.34
14	0.00	0.00	6.64	160.00	153.36	182.94	176.30
15	0.00	0.00	6.64	110.00	103.36	142.75	136.11
16	0.00	0.00	6.64	85.00	78.36	111.73	105.09
17	0.00	0.00	6.64	60.00	53.36	87.78	81.14
18	0.00	0.00	6.64	55.00	48.36	69.29	62.65
19	0.00	0.00	6.64	50.00	43.36	55.01	48.37
20	0.00	0.00	6.64	50.00	43.36	43.98	37.34
21	0.00	0.00	6.64	40.00	33.36	35.47	28.83
22	0.00	0.00	6.64	35.00	28.36	28.90	22.26
23	0.00	0.00	6.64	30.00	23.36	23.83	17.19
24	0.00	0.00	6.64	25.00	18.36	19.91	13.27
25	0.00	0.00	6.64	15.00	8.36	16.89	10.25
Sum (ordinates)	27.23	12.27	166.00	3815.00	3649.00	3552.98	3386.98
Volume (mm)	27.23	12.27	0.73	16.68	15.95	15.53	14.80

performance to some extent only. For completeness, here it is in order to show the variation of S (or CN) within a storm event, in what follows.

**e) Variation of Curve Number within an Event**

The computation of potential maximum retention S and Curve Number (CN) is shown in Table 7 for an example event 1 of Jhandoonala watershed. The computed CN-values are rounded off to a near integer value. It is visible that as the time duration of the storm increases, the S decreases and CN increases. The CN varies from 3-15. These results are consistent with the comprehensive analysis of Mishra and Singh (2000) describing the physical significance of S using infiltration data.



**TABLE 7. VARIATION OF S AND CN WITHIN AN ECAMPLE EVENT (EVENT 1 OF JHANDOO NALA WATERSHED)**

Time (min)	Observed Rainfall (mm)	Cumulative Rainfall (mm)	Uniform Rainfall Intensity, $i_o$ (mm/min)	k ( $\text{min}^{-1}$ )	$S = i_o/k$ (mm)	CN=25400/(S+254)
10	60	60	6.00	0.000757	7926	3
20	75.81	135.81	6.79	0.000757	8970	3
30	69.54	205.35	6.85	0.000757	9042	3
40	24	229.35	5.73	0.000757	7574	3
50	9	238.35	4.77	0.000757	6297	4
60	9	247.35	4.12	0.000757	5446	4
70	7.8	255.15	3.65	0.000757	4815	5
80	3	258.15	3.23	0.000757	4263	6
90	1.2	259.35	2.88	0.000757	3807	6
100	1.2	260.55	2.61	0.000757	3442	7
110	3.6	264.15	2.40	0.000757	3172	7
120	3	267.15	2.23	0.000757	2941	8
130	6	273.15	2.10	0.000757	2776	8
140	3	276.15	1.97	0.000757	2606	9
150	2.4	278.55	1.86	0.000757	2453	9
160	2.4	280.95	1.76	0.000757	2320	10
170	2.4	283.35	1.67	0.000757	2202	10
180	1.8	285.15	1.58	0.000757	2093	11
190	1.8	286.95	1.51	0.000757	1995	11
200	1.2	288.15	1.44	0.000757	1903	12
210	3	291.15	1.39	0.000757	1831	12
220	1.8	292.95	1.33	0.000757	1759	13
230	1.2	294.15	1.28	0.000757	1689	13
240	1.2	295.35	1.23	0.000757	1626	14
250	1.2	296.55	1.19	0.000757	1567	14
260	0.6	297.15	1.14	0.000757	1510	14
270	0	297.15	1.10	0.000757	1454	15

## CONCLUSION

An SCS-CN based short-term rainfall-runoff model was developed and applied to the seventeen events of Jhandoo Nala watershed of Himalaya, affected by mining activities, and seven events of 3F sub-zone watershed of river Godavary. The parameters were computed employing the Marquardt algorithm of least squares using the standard error and coefficient of determination criteria of minimising errors. The events of Jhandoo Nala watershed yielded the standard errors varying from 0.0031 to 0.0681 and  $r^2$  from 0.3975 to 0.9782. Out of 17 events, 13 events were simulated with  $r^2$  greater than 0.70, exhibiting a reasonably good performance of the model. Similarly, 3 events of 3F sub-zone watershed yielded  $r^2 > 0.7$  and 5 events yielded  $r^2 > 0.6$ , showing reasonably good performance. The values of computed peak discharge and time to peak discharges also, in general, matched closely with the observed ones. The volumetric analysis supported by example applications exhibited encouraging results of simulation. The major advantage of the developed model is that the mass is conserved almost fully.

## REFERENCES

1. Andrews, R.G., The use of relative infiltration indices in computing runoff, in *Rainfall-Runoff Relationship*, edited by V.P. Singh, Water Resour. Pub., Littleton, Colorado 80161, 1954.
2. Chen Cheng-lung, An evaluation of the mathematics and physical significance of the soil conservation service curve number procedure for estimating runoff volume, in *Rainfall-Runoff Relationship*, edited by V.P. Singh, Water Resour. Pub., Littleton, Colo. 80161, 1982.
3. Dunne, T. and R.D. Black, Partial area contributing to storm runoff in a small New England watershed, *Water Resources Res.*, 6(5), 1286-1311, 1970.
4. Hawkins, R.H., Asymptotic determination of runoff curve numbers from data, *J. Irrig. and Drain. Engrg.*, ASCE, Vol. 119, No. 2, pp. 334-345, 1993.
5. Hewlett, J.D. and A.R. Hibbert, Factors affecting the response of small watersheds to precipitation in humid area, Proc., Int. Symp. on *Forest Hydrology*, edited by W.E. Sopper and H.W. Lull, Pergamon Press, Oxford, England, 275-290, 1967.
6. Hjelmfelt, A.T., Jr., Investigation of curve number procedure, *J. Hydraul. Engrg.*, Vol. 117, No. 6, pp. 725-737, 1991.
7. Katiyar, A.K. (1997), 'Rainfall runoff modelling of hilly watersheds,' Ph.D. Dissertation, Dept. of Hydrology, University of Roorkee, Roorkee-247 667, UP, India.
8. McCuen, R.H., *A Guide to Hydrologic Analysis Using SCS Methods*, Prentice-Hall Inc., Englewood Cliffs, New Jersey, 1982.
9. Mein, G. R. and C.L. Larson, Modelling the infiltration component of the rainfall-runoff process, Water Resources Research Center, University of Minnesota, Minneapolis, Minnesota, 1971.
10. Miller, N. and R. Cronshey, Runoff curve numbers, the next step, Proc. Int. Conf. on *Channel Flow and Catchment Runoff*, Univ. of Virginia, Va., 1989.
11. Mishra, S.K. and V.P. Singh, Another look at the SCS-CN method, *J. Hydrologic Engineering*, ASCE, Vol. 4, No. 3, pp. 257-264, 1999a.

12. Mishra, S.K. and V.P. Singh, 'Behaviour of SCS-CN method in C-I<sup>n</sup>-λ spectrum,' Proc., "Hydrologic Modeling", Int. Conf. on Water, Environment, Ecology, Socio-economics, and Health Engineering, Seol Nat. Uni., Korea, Oct. 18-21, pp. 112-117, 1999b.
13. Mishra, S.K. and V.P. Singh, 'The SCS-CN method revisited,' Submitted to J. Hydrology, 2000.
14. Mishra, S.K., R.D. Singh, and R.K. Nema, Application of a modified SCS-CN method,' Int. Conf. on *Hydrology*, Central Board of Irrigation and Power, New Delhi, Dec. 8-10, 1998.
15. Mishra, S.K. (2000), 'SCS-CN based long term hydrologic simulation,' Tech. Rep., National Institute of Hydrology, Roorkee-247 667, UP, India.
16. Mockus, V., Estimation of total (peak rates of) surface runoff for individual storms, Exhibit A of Appendix B, Interim Survey Report Grand (Neosho) River Watershed, USDA, Dec. 1, 1949.
17. Mockus, V., Letter to Orrin Ferris, March 5, 6p, 1964, reference in Rallison, R.E, Origin and evolution of the SCS runoff equation, Proc., ACSE Symp. *Watershed Management*, Boise, Idaho, July, 1980.
18. Ponce, V.M., and R.H. Hawkins, Runoff curve number: Has it reached maturity?, J. *Hydrolog. Engrg.*, ASCE, Vol. 1, No. 1, pp. 11-19, 1996.
19. Ponce, V.M. (1989), 'Engineering Hydrology,' Prentice Hall, Englewood, New Jersey.
20. Rallison, R.E, Origin and evolution of the SCS runoff equation, Proc., ASCE Symp. *Watershed Management*, Boise, Idaho, July, 1980.
21. Rallison, R.E and N. Miller, Past, present, and future SCS runoff procedure, in *Rainfall-Runoff Relationship*, (ed.) V.P. Singh, Water Resour. Pub., Littleton, Colorado 80161, 1982.
22. Ritter, J.B. and T.W. Gardner, Runoff curve numbers for reclaimed surface mines in Pennsylvania, J. *Irrig. and Drain. Engrg.*, ASCE, Vol. 117, No. 5, pp. 656-666, 1991.
23. Sherman, L.K., Hydrograph of runoff, Physics of the Earth, IX, *Hydrology*, edited by O.E., Meinzer, McGraw-Hill, New York, N.Y., 1942.

24. Sherman, L.K., The unit hydrograph method, Physics of the Earth, IX, *Hydrology*, edited by O.E., Meinzer, McGraw-Hill, New York, N.Y., 1949.
25. Singh, V.P., *Hydrologic Systems, Vol. I: Rainfall Runoff Modeling*, Prentice Hall Inc., Englewood Cliffs, New Jersey, 1988.
26. Soil Conservation Service, *Hydrology, National Engineering Handbook*, Supplement A, Section 4, Chapter 10, Soil Conservation Service, USDA, Washington, D.C., 1956, 1964, 1985.
27. Steenhuis, T.S., M. Winchell, J. Rossing, J.A. Zollweg, and M.F. Walter, SCS runoff equation revisited for variable-source runoff areas, *J. Irrig. & Drainage Engg.*, ASCE, 121(3), pp. 234-238, 1995.
28. Svoboda, A., Changes in flood regime by use of the modified curve number method, *Hydrol. Sci. J.*, Vol. 36, No. 5/10, pp. 461-470, 1991.
29. Tyagi, A., R.D. Singh, and R.K. Nema (1995), 'Derivation of Nash model based unit hydrograph using Marquardt algorithm,' Hindi, Nat. Conf., on Hydrology and Water Resources, National Institute of Hydrology, Roorkee, UP, India, Dec. 15-16.

**DIRECTOR**  
**COORDINATOR**  
**DIVISIONAL HEAD**  
**SCIENTIST**  
**STENO**

**DR. S.M. SETH**  
**SH. R. D. SINGH**  
**DR. S.K. MISHRA**  
**DR. S.K. MISHRA**  
**T.P. PANICKER**